NASA TECHNICAL MEMORANDUM NASA TM-75447

DYNAMIC STALL: AN EXAMPLE OF STRONG INTERACTION BETWEEN VISCOUS AND INVISCID FLOWS

Jean-Jacques Philippe

Translation of "Le déchrochage dynamique, Un exemple d'interaction forte èntre écoulements visqueux et non-visqueux," ONERA, Chatillon-sous-Bagneux, Hauts-de-Seine, France. (NATO, AGARD, Symposium on Unsteady Aerodynamics, Ottawa, Canada, September, 26-28, 1977). ONERA, TP No. 1977-135, 1977. 22 pp.

(NASA-TM-75447) DYNAMIC STALL: AN EXAMPLE OF STRONG INTERACTION BETWEEN VISCOUS AND INVISCID FLOWS (National Aeronautics and Space Administration) 57 p HC A04/MF A01 CSCL 20D G3/34 N78-32384 Unclas 31611

NATIONAL AERONAUTICS AND SPACE ADMINISTRATION
WASHINGTON, D. C. 20546 SEPTEMBER 1978

STANDARD TITLE PAGE

1. Report No. NASA TM-75447	2. Government Accession No.	3. Recipient's Catalog No.
4. Title and Subtitle DYNAMIC STALL:— AN EXAMPLE OF STRONG INTERACTION BETWEEN VISCOUS AND INVISCID FLOWS		5. Report Date September 1978
		6. Performing Organization Code
7. Author(s) J.-J. Philippe		8. Performing Organization Report No.
		10. Work Unit No.
9. Performing Organization Name and Address SCITRAN Box 5456 Santa Barbara, CA 93108		11. Contract or Grant No. NASW-3198
		13. Type of Report and Period Covered Translation
12. Sponsoring Agency Name and Address National Aeronautics and Space Administration Washington, D.C. 20546		14. Sponsoring Agency Code

15. Supplementary Notes

Translation of: "Le déchrochage dynamique, Un exemple d'interaction forte entre écoulements visqueux et non-visqueux," ONERA, Chatillon-sous-Begneux, Hauts-de-Seine, France. (NATO, AGARD, Symposium on Unsteady Aerodynamics, Ottawa, Canada, September, 26-28, 1977). ONERA, TP No. 1977-135, 1977. 22 pp. (A78-24467)

16. Abstract

This paper surveys the phenomena concerning profiles in dynamic stall configuration, and more specially those related to pitch oscillations. The most characteristic experimental results on flow separations with a vortex character, and their repercussions on local pressures and total forces are analyzed. Some aspects of the methods for predicting flows with the presence (or not) of boundary layer separation are examined, as well as the main simplified methods available to date for the calculation of total forces in such configurations (Author)

17. Key Words (Selected by Author(s))	18. Distribution Statement Unclassified — Unlimited

19. Security Classif. (of this report) Unclassified	20. Security Classif. (of this page) Unclassified	21. No. of Pages 57	22.

DYNAMIC STALL: AN EXAMPLE OF STRONG INTERACTION BETWEEN VISCOUS AND INVISCID FLOWS by Jean-Jacques Philippe

Office National d'Etudes et de Recherches Aérospatiales (ONERA)
(National Office for Aerospace Studies and Research)
92320, Châtillon, France

This paper reports on the phenomena associated with airfoils in a dynamic stall configuration with emphasis on those associated with airfoils oscillating in pitch. The most characteristic experimental results of flow separations of a vortex nature and their impact on local pressures and total forces are analyzed. A few aspects of the methods for predicting flows in the presence (or absence) of boundary-layer separation are examined, as well as the main simplified methods available to date for computing the total forces in such configurations.

1 - INTRODUCTION

The term "dynamic stall" includes a group of aerodynamic phenomena which take place when an airfoil, a blade section, a wing or an aircraft is subjected to time-varying aerodynamic conditions which lead to drops in lift or sudden increases in the pitch moment which are two characteristics of stall configurations.

For example, during certain helicopter flying configurations, the rotor blades can be periodically subjected to dynamic reattachment and stall. Indeed, incidence angles on the receding rotor blade can be far greater than the airfoil steady stall angles whereas incidence angles of the forward-moving blade are low.

To illustrate the major phenomena associated with a change of incidence angle of the airfoil about its stall incidence angle, Figure 1 extracted from reference 1 shows that, by comparison with steady aerodynamic characteristics, the airfoil can:

- reach lift levels much higher than those obtained in a stationary flow while being the center of major separations with organized vortices shown in the figure by means of smoke released at various points on the airfoil,
- display, during the critical phase when the airfoil is subjected to separations, very high-level pitching moments (moment stall preceding lift stall),
- be subjected to aerodynamic forces such that the work by these forces having become positive tends to make the incidence motion unstable.

In what follows, we will analyze the various aspects of this phenomenon and we will cover what we know on:

- unsteady viscous flows with separation and reattachment over an airfoil moving cyclically,
- the consequences of such flows on local pressures and on total unsteady aerodynamic forces,
- computation methods for flows about the airfoils that can be applied to dynamic stall configurations,
- practical methods that manufacturers can use to evaluate aerodynamic performances under such conditions.

The author was greatly helped by W.J. McCroskey and his USAAMRDL team from the Ames laboratory in the preparation of this document, thanks to the work performed jointly in the area of dynamic stall and to summary reports on this subject (references 1 and 2). Let them be thanked here. for their assistance.

2 - ANALYSIS OF THE PRIMARY CHARACTERISTIC OF DYNAMIC STALL

2.1. - The vortex nature of separation flows.

Displays of flows about airfoils make it possible to analyze the type and structure of the flows on which depend the aerodynamic characteristics of the airfoils. ONERA has a hydrodynamic tunnel which proved to be a very useful investigation tool for studies in unsteady aerodynamics (reference 3).

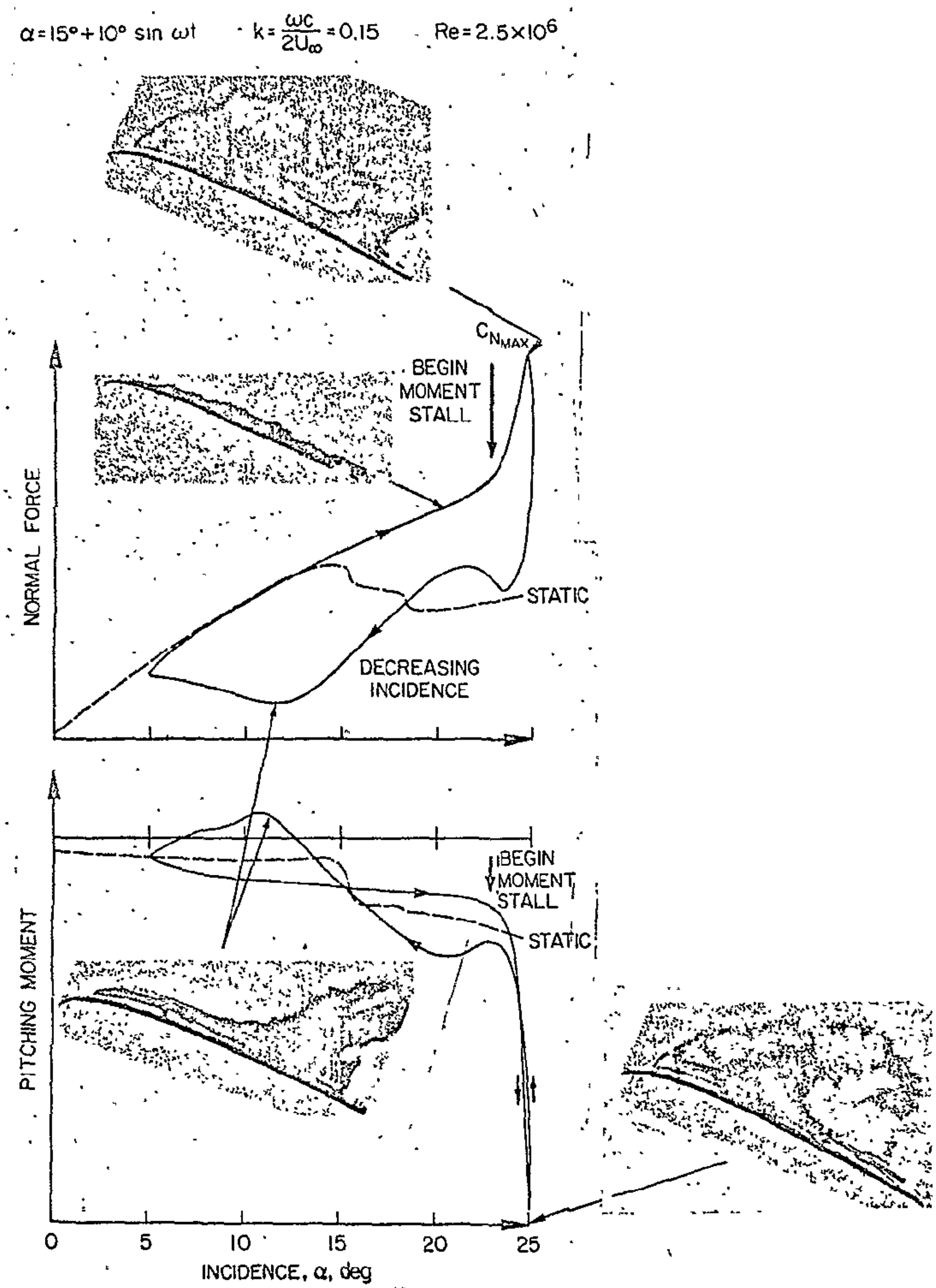

Figure 1 - Example of the development of forces and pitching moments in steady and unsteady flow.

Figure 2 shows the NACA 0012 profile with pitch harmonic oscillations on both sides of the incidence angle for steady flow stall. When the incidence angle increases, we can greatly exceed this incidence without seeing the separation that is noticeable on the airfoil (photo 2a). However, there is a time in the cycle when large separations take place; these display a highly vortex nature. As we can see in Figure 2b, a vortex formed near the leading edge moves toward the trailing edge of the airfoil.

ORIGINAL PAGE IS OF POOR QUALITY

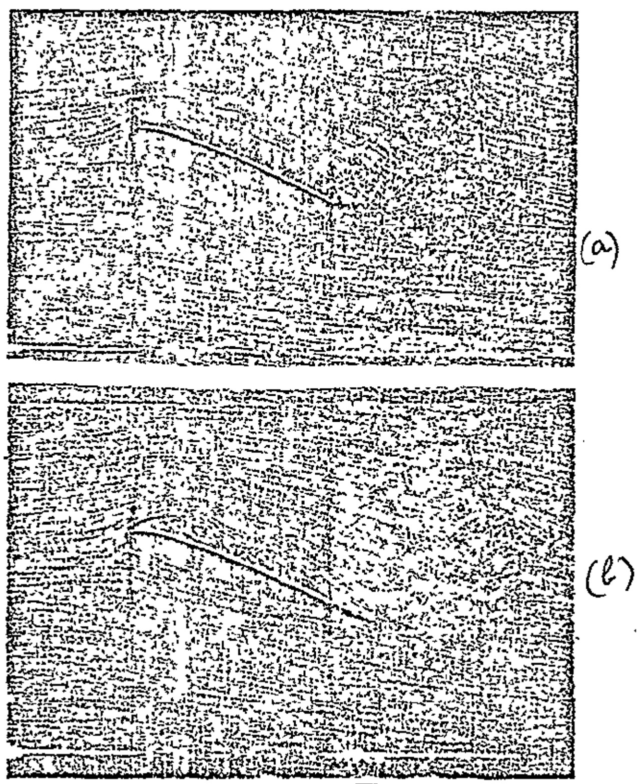

Figure 2 - Pitch Harmonic Oscillations.
$\alpha = 12.5^{\circ} + 5^{\circ} \sin \omega t$; k=0.95; $Re_c = 6000$
Displays obtained at the ONERA hydrodynamic tunnel

Figure 3 shows the same airfoil set to a fixed geometric incidence angle close to the unsteady-flow stall angle but with harmonic oscillation beats (vertical translations of the airfoil). The rising phase of the airfoil retards the appearance of stall on the airfoil as during the phase of increasing incidence of the airfoil oscillating in pitch (photo 3a). When separations appear on the airfoil, they also have a vortex character. We then observe, from a point close to the leading edge, the formation and then the upstream motion of a vortex (Photograph 3b).

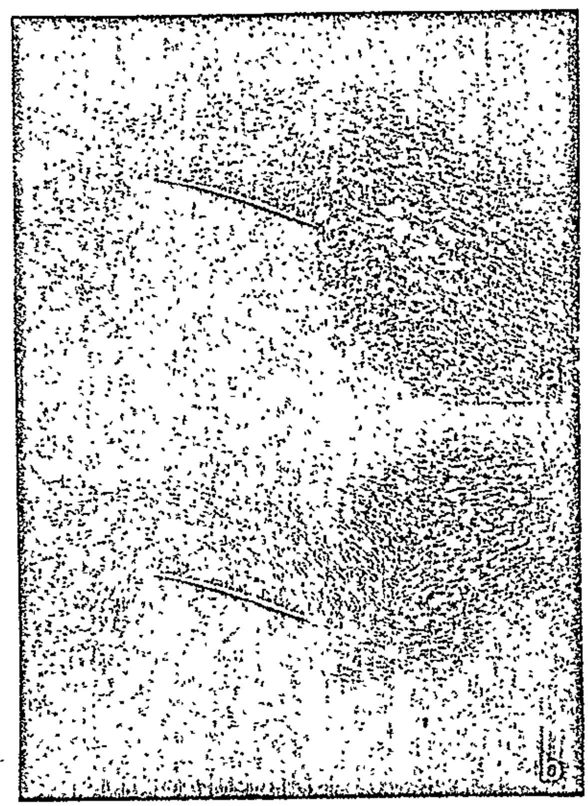

Figure 3 - Beat Harmonic Oscillations (Up-and-Down Motion)

$\alpha = 12.5^{o}$; $\Delta z = 0.25\ c \sin \omega t$; $k = 0.95$; $Re_c = 6000$

Displays obtained at the ONERA hydrodynamic tunnel.

Figure 4 still involves the same profile set to a fixed geometric incidence angle but it is driven through a harmonic back and forth motion (horizontal translations of the airfoil). The displays show that the separated area over the top of the advancing airfoil is the center of a continuous source of vortices carried away by the flow (Photograph 4a) while, in the case of the receding airfoil (Photograph 4b), the vortex nature is more diffuse.

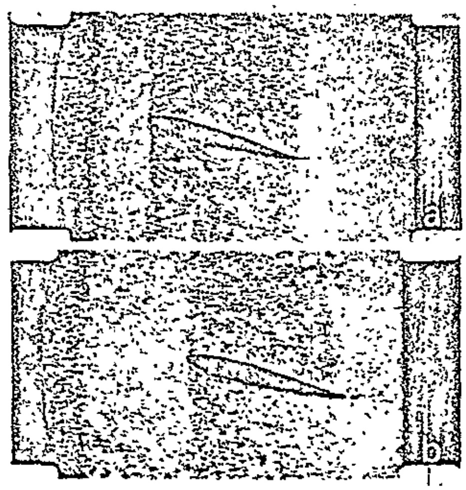

ORIGINAL PAGE IS OF POOR QUALITY

Figure 4 - Back-and-forth Harmonic Oscillations.
$\alpha = 12.5^{\circ}$; $\Delta x = 1.5\ c \sin \omega t$; $k = 0.1075$; $Re_c \simeq 6000$
Displays obtained at the ONERA hydrodynamic tunnel

These displays made in water involve low Reynolds numbers (at the chord) in the order of 6000. The USAAMRDL of the Ames Laboratory has a hydrodynamic tunnel that makes studies possible with Reynolds numbers in the order of 0.5×10^6 (Reference 4). Displays are made using hydrogen bubbles produced through electrolysis using a technique developed by K.W. McAlister of the US Army AMRDL of Ames. The photographs in Figure 5 extracted from a document to be published (Reference 5) show the good quality of the displays obtained in that manner with a modified NACA 0012 airfoil oscillating in pitch.

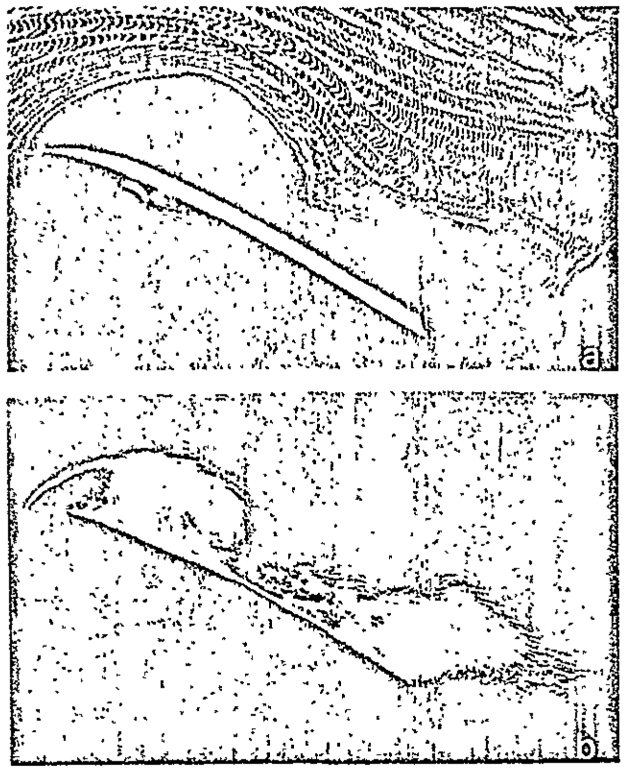

Figure 5 - Displays using hydrogen bubbles (Ames USAAMRDL).
NACA 0012 airfoil oscillating in pitch.
$\alpha = 15^{o} + 10^{o} \sin \omega t$; photographs taken with $\alpha = \alpha Max$

Displays made in the air by generating smoke from different points on the airfoil (Figure 1) are also very interesting in subsonic flow. During a very detailed study of dynamic stall, the Ames USAAMRDL built a NACA 0012 airfoil with a 1.20 meter chord for its 7 x 10ft wind tunnel (References 6 and 7). The tests covered Reynolds numbers ranging from 1 to 3.5×10^{6} for the NACA 0012 airfoil and for other airfoils obtained by changing the shape of the leading edge of that same airfoil.

A movie to be presented during this symposium shows:

- a case of leading edge dynamic stall of the type called "bursting of the leading edge laminar bubble" when the radius of the leading edge of the NACA 0012 airfoil is reduced to a 0.4% instead of the standard 1.58,

- a case of trailing edge stall of the type called "gradual flow reversal of trailing edge separations toward the leading edge" when the NACA 0012 airfoil is equipped with a cambered extension designed by ONERA,
- a case of complex stall for the reference NACA 0012 airfoil as it involves sudden turbulent leading edge stall preceded by a non-negligible reversed flow of trailing edge separations.

We will cover in detail these different types of dynamic stall in the next paragraph but it is to be noted that in each of these cases, we have, in the critical phase of generalized separation, the presence of vortices that are more or less organized and complex as shown in the photos of Figure 6.

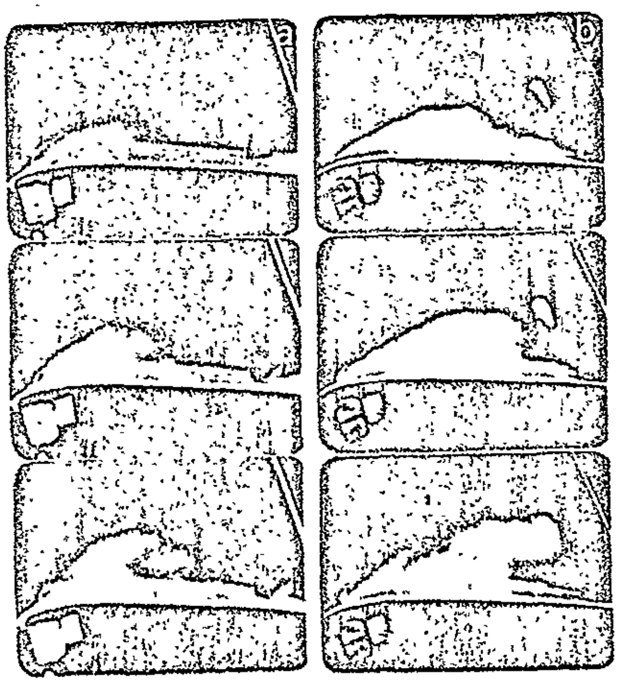

Figure 6 -Evolution of separations of a vortex nature with an oscillating airfoil.
a) NACA 0012 with a reduced leading edge radius
b) NACA 0012 with a cambered extension
$Re_c = 2.5 \times 10^6$; $\alpha = 15^\circ + 10^\circ \sin \omega t$; k=0.15; Ames USAAMRDL tests.

2.2 - Unsteady Separations of the Turbulent Boundary Layer.

Heated films are good detectors of heat flux. The convected flux depends very much on the laminar, turbulent or separated condition of the boundary layer at a perpendicular angle to the heated film (reference 8).

Thus, as shown in figure 7, during S10 wind tunnel tests at the Toulouse Aeronautical Test Center, we showed a gradual flow reversal of the turbulent separation originating from the NACA 0012 trailing edge (with a cambered extension to the airfoil) oscillating in pitch on both sides of its steady stall angle of attack (Reference 9). This phase precedes the generalized separation phase with vortices as described in the preceding paragraph.

The same type of information can be obtained with heated wires placed very close to the top of the airfoil. This technique has been used by the Ames USAAMRDL (Reference 10) during the test program with the NACA 0012 airfoil and its derivatives, a test program already mentioned above. Figure 8, extracted from reference 2, shows the development of separations from various airfoils tested against time or the geometric incidence angle of the airfoils. To obtain this figure, we have made the point where separation takes place the same as the point where reverse flow appears for the first time, a procedure that is not very rigorous.

However, it is clear that, under identical conditions of oscillations in pitch:

- the NACA 0012 airfoil with a reduced leading edge sees separations take shape and propagate mainly from the leading edge to the trailing edge,
- the NACA 0012 airfoil with a cambered extension sees separations take shape and propagate from the trailing edge to the leading edge,

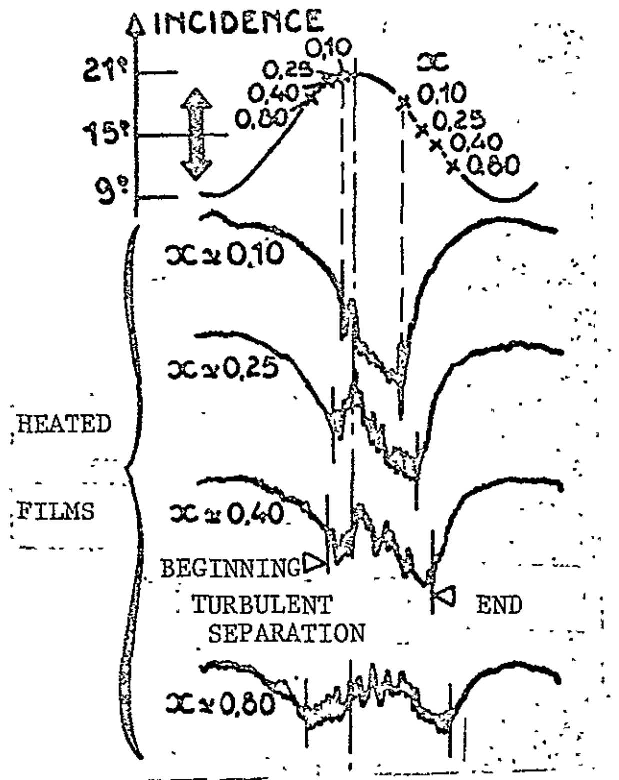

Figure 7 - Evolution of turbulent separations with a NACA 0012 airfoil with a cambered extension. M=0.2; k=0.114; Re_c=1.9 x 10^6.

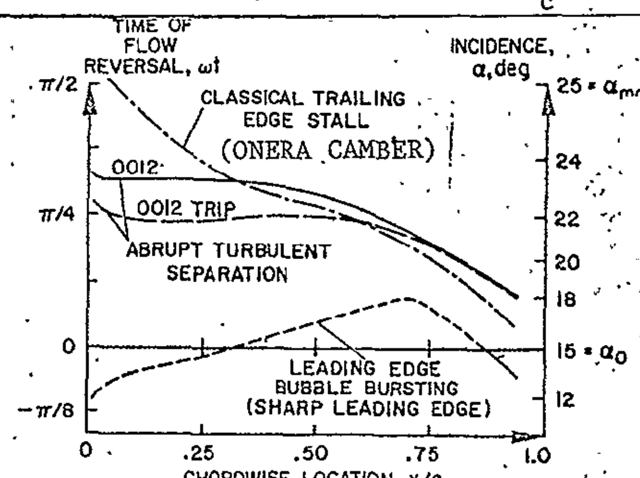

Figure 8 - Evolution of turbulent separations with an oscillating airfoil. $\alpha=15^{\circ}+10^{\circ}\sin\omega t$; k=0.15; Re=2.5x$10^6$.

- the NACA 0012 airfoil first sees a trailing edge separation move back toward the leading edge then sees a sudden separation take place from the leading edge before trailing edge separations can reach the leading edge whether the transition has been triggered or not.

These separations of the turbulent boundary layer depend, as in stationary flow, on many parameters:

- those that condition the value of the local pressure gradient:
  - the airfoil itself as illustrated in the preceding Figure 8,
  - the average incidence angle and the amplitude of oscillations in pitch,
  - the reduced oscillation frequency since the time derivatives of the airfoil incidence angle are directly proportional to it.

Figure 9, derived from Figure 26 of reference 10, illustrates the effect of this parameter. The higher the reduced oscillation frequency, the later separations appear. This delays the generalized separation over the airfoil by the same amount.

- those associated with viscosity:
  - the Reynolds number
  - the location of the boundary layer transition, whether created naturally or artificially.

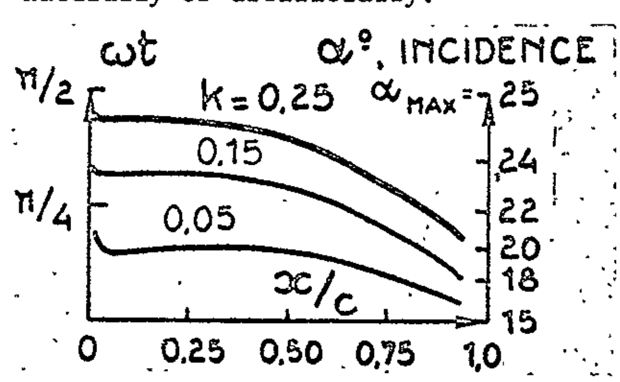

Figure 9 - Effect of the reduced frequency on the evolution of separations. NACA 0012. $\alpha=15^{\circ}+10^{\circ}\sin\omega t$

Figure 10, derived from Figure 32 in reference 10 illustrates the effect of the Reynolds number. The higher that number, the later the separations appear and develop.

The effect of upstream conditions on separation will be discussed in Paragraph 4.3.

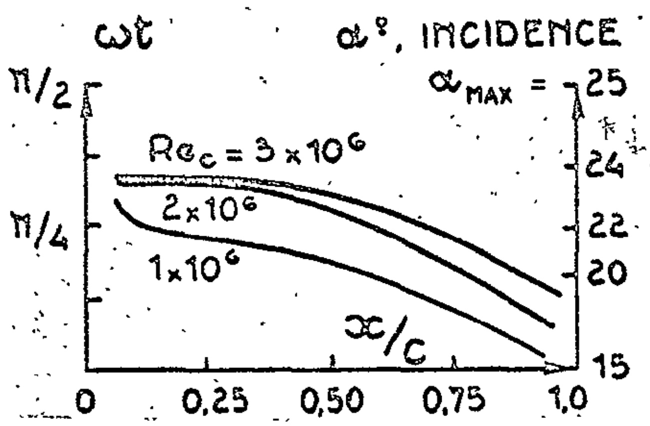

Figure 10 - Effect of the Reynolds number on the evolution of separations. NACA 0012. $\alpha=15^{\circ}+10^{\circ}\sin\omega t$; $k=0.15$.

x = abscissa of the separation point.

---

3 - TOTAL FORCES AND LOCAL PRESSURES ON AIRFOILS IN A DYNAMIC STALL.

3.1. - Typical Example of an Airfoil with Harmonic Oscillations in Pitch.

Figure 11, extracted from reference 2, picks up the lift and pitching moment cycles of NACA 0012 airfoil oscillating in pitch already depicted in Figure 1 but it links the main consequences of dynamic stall described in detail in the preceding paragraph to different times in the incidence cycle.

We will particularly note that the lift of the airfoil continues to increase with the incidence angle, way beyond the maximum value obtained in stationary flow and this in spite of the presence of reversed flow inside an increasingly turbulent and thick boundary layer over a large section of the chord of the airfoil (a). A vortex is generated near

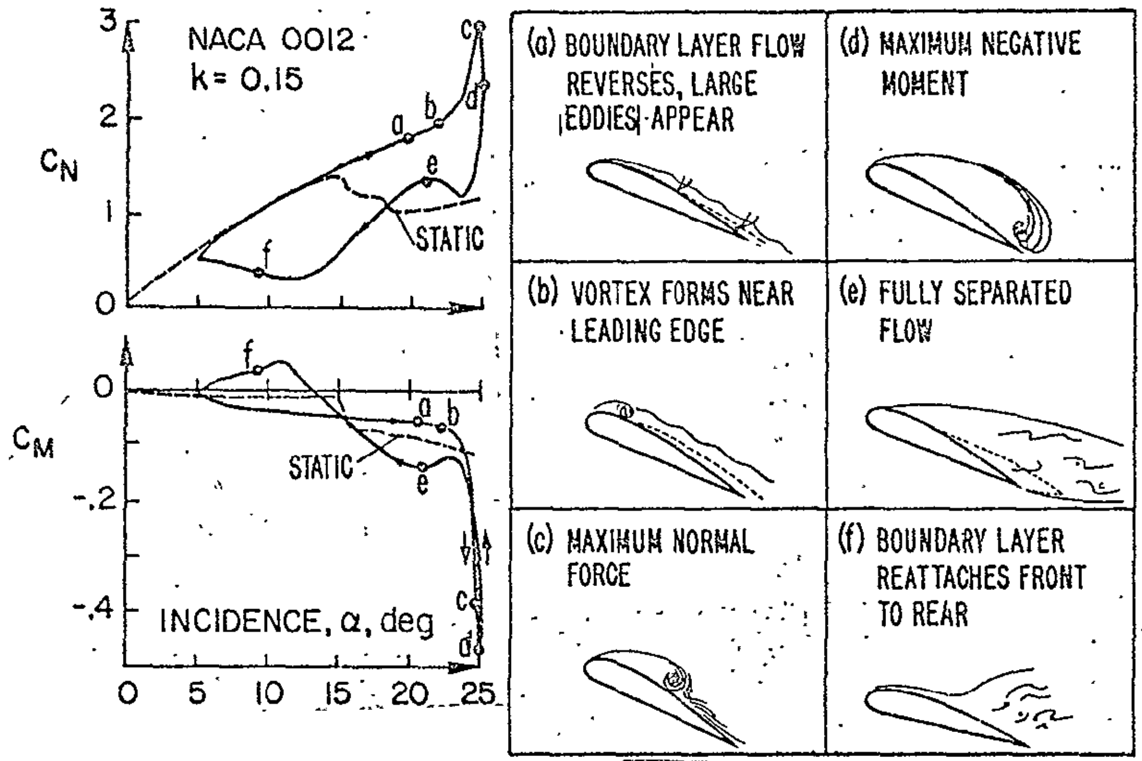

Figure 11 - Main events associated with the NACA 0012 airfoil in a dynamic stall configuration. Re = 2.5×10^6.

the leading edge (b) and the lift continues to increase with increased speed with a greater incidence angle. The departure of the vortex toward the trailing edge causes a moment stall of the airfoil but the lift stall (c) takes place only a little later when the vortex has gone, in this particular case, a little beyond the half-chord of the airfoil. Negative pitching moments (Cm < 0) can take take much higher values than during steady flow stalls and this is due primarily to loads induced by the vortex during its motion. The maximum negative moment corresponds to the passage of the vortex over the trailing edge (e). The incidence angle continues to decrease, the boundary layer finally reattaches itself to the airfoil, starting with the leading edge (f) but we find a non-separated airfoil only at incidence angles much lower than the incidence angles for stall in a steady flow.

Absolute pressure measurements made during tests conducted by the Ames USAAMRDL are very useful in following the evolution of phenomena associated with the presence, development and motion of vortices that are characteristic of dynamic stall.

Thus, Figures 12 and 13 extracted from a document to be published (reference 11) show that:

- pitch stall (b) is caused by the sudden reaction of high pressure drops at the leading edge (a) (Figure 12) but is slightly preceded by that drop. The pressure drop takes place earlier but less suddenly if we trigger the transition artificially. Lift stall (c) takes place only a little later.

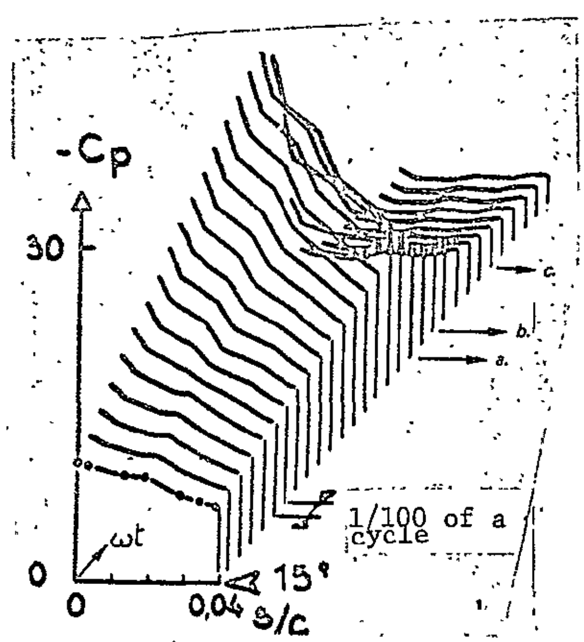

Figure 12 - Evolution of pressures in the leading edge area. Case of the NACA 0012 airfoil in a free transition.
$\alpha = 15^{o} + 10^{o} \sin \omega t$; k=0.15.

- the vortex moves along the topside of the airfoil generating local pressure drops as it moves (Figure 13); the maximum pressure drops make it possible to locate the vortex; we find that the displacement velocity of this vortex is generally less than half the flow velocity at an infinite upstream distance. A detailed study of this phenomenon is also made in reference 12 by F.O. Carta, using tests made by Sikorsky in 1972 using a NACA 0012 airfoil.

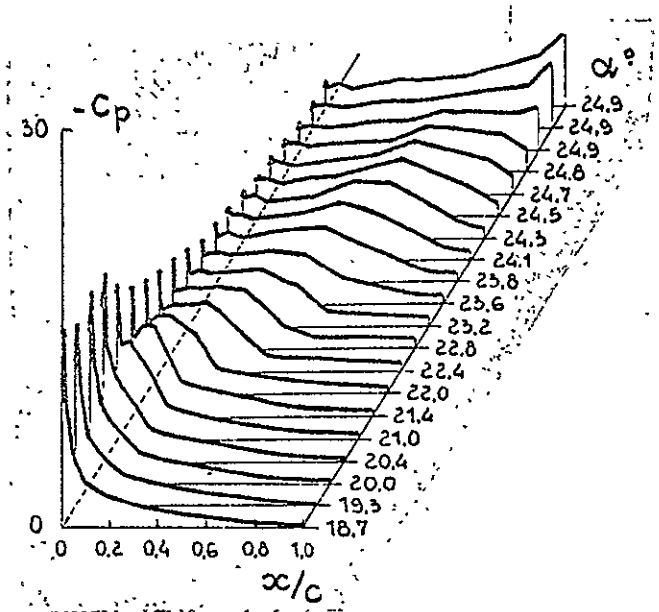

ORIGINAL PAGE IS
OF POOR QUALITY

Figure 13 - Effect of the passing vortex on pressure distributions. Case of the NACA 0012 airfoil with a fixed transition. $k = 0.15$; $\alpha = 15^{\circ} + 10^{\circ} \sin \omega t$.

Knowing the local absolute pressures makes it also possible to follow the evolution of pressure drags. Figure 14 shows the pressure drag cycle along the axes associated with the model.

The absolute pressure measurement technique has also been used by other researchers such as A.G. Parker (reference 13) and previously by R.I. Windsor (reference 14); these works are very useful as they also provide

ORIGINAL PAGE IS OF POOR QUALITY

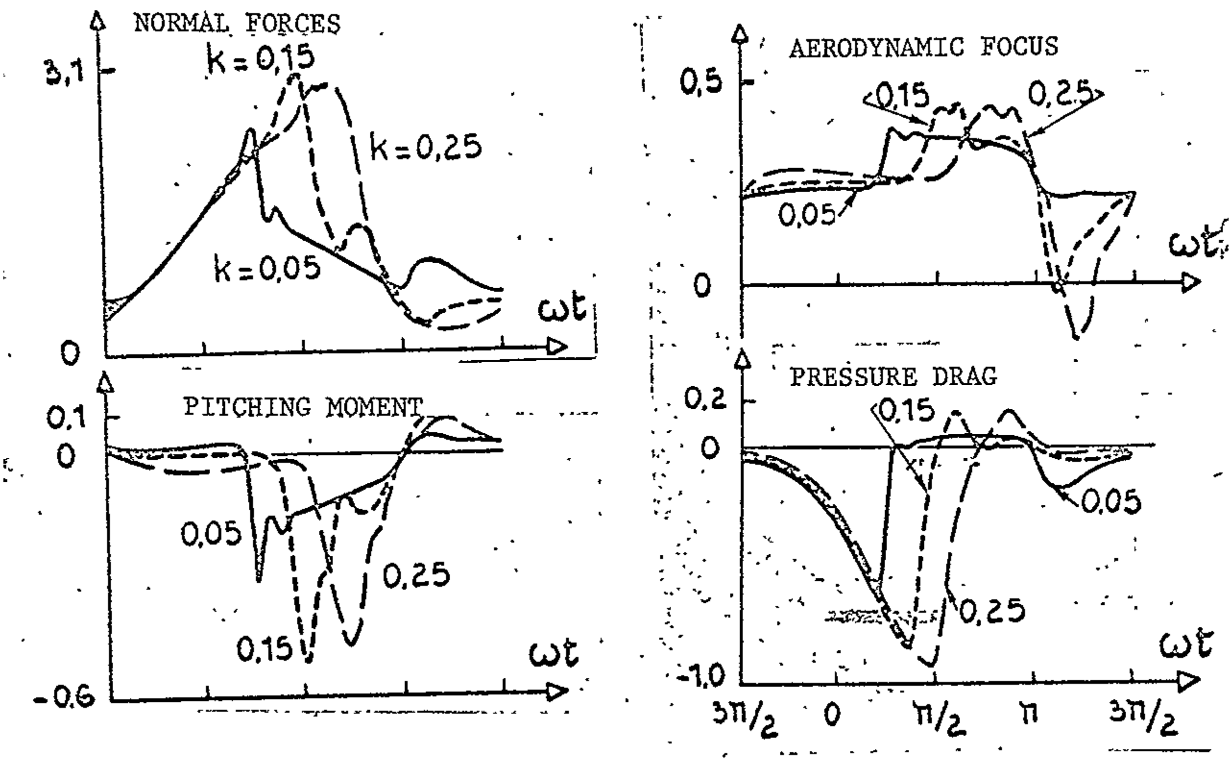

Figure 14 - Effect of the reduced frequency. Case of the NACA 0012 airfoil with a free transition.
$\alpha = 15^{\circ} + 10^{\circ} \sin \omega t$.

---

a basis for comparison for developing computation methods for unsteady flows in the presence or absence of dynamic stall.

3.2. - Characteristic aerodynamic value for airfoils with harmonic oscillations in pitch.

The typical previous example reveals a certain number of aerodynamic values for which it is interesting to know the evolution as a function of oscillation parameters. The following are mainly involved:

- the maximum lift reached by the airfoil during an oscillation since it quantitatively reveals the beneficial consequence of the delay in the stall as noted experimentally,
- the maximum negative moment obtained during the critical phase of dynamic stall since it can quantitatively reveal the penalty level of dynamic stall.

Another significant point of dynamic stall configurations involves energy transfers between the airfoil and the airflow which, therefore, condition aerodynamic stability.

The inside area of the pitching moment cycles as a function of incidence angles is proportional to the work of the aerodynamic forces ($\oint C_m \, d\alpha$) If the cycle is accomplished in a counter-clockwise direction, the aerodynamic damping is positive and the motion is stable. On the other hand, if the cycle is accomplished in a clockwise direction, the work by the aerodynamic forces is positive, the aerodynamic damping is negative and this can lead to a tension instability of the blade.

The very complete tests conducted in 1968 and 1969 by Boeing-Vertol with 4 airfoils (references 16 and 17) equipped with differential pressure sensors and moving in pitch and up and down with a varying reduced frequency showed that the amplitude and the average incidence of the oscillations and the Mach number make it possible to determine the effect of these parameters on the unsteady aerodynamic performances of the airfoils.

There is no question here of providing all of the typical results obtained but simply to bring the attention to the primary effects, particularly the following:
- the average incidence of the oscillation and the associated amplitude as the effects are very different depending on whether the range of angles examined is located ahead of, on both sides or behind the steady

flow stall incidence angle of the airfoil. Figure 15 shows an example of the cycles obtained. We will note that it is in an oscillation on both sides of the steady flow stall incidence angle that the effects are the most noticeable and that they lead to large maximum lifts and to the possiblity of instability in pitch. When the airfoil oscillates continuously in separated flow, with high average incidence angles, motion becomes stable again; however, generally speaking, this takes place with high values of negative pitching moments.

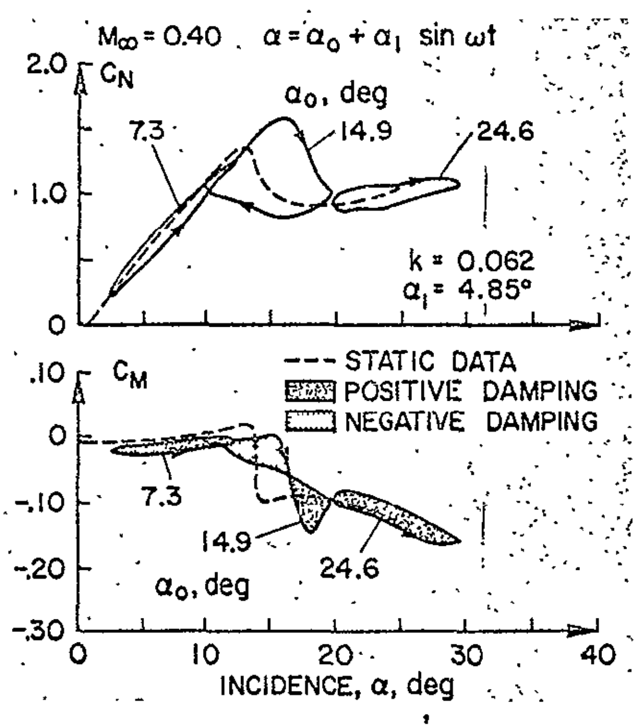

Figure 15 - Cycles of the forces and moments obtained with a Vertol 23010 airfoil with harmonic oscillations in pitch ($Re_c = 4.8 \times 10^6$).

- the Mach number, since as soon as this parameter increases a little and we have high incidence angles, problems associated with compressibility appear. Figure 16, extracted from reference 2, shows the cycles obtained with different Mach numbers and with average incidence angles that are slightly greater than the corresponding stall incidence angles for steady

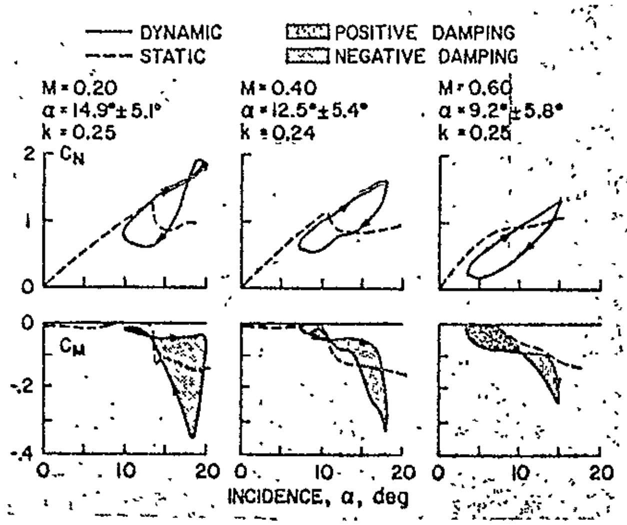

Figure 16 - Effect of the Mach number on the unsteady flow characteristics of the NACA 0012 airfoil.

---

flow. If the general shape of the cycles remains the same, we will note that the maximum lift decreases with the Mach number and that, in general, the maximum negative moments are less significant at a high Mach number. We will note particularly the tendency of pitch instabilities at a high Mach number to disappear. This can be caused by a weaker generation of vortices when the shock wave is located near the leading edge of the airfoil.

These tests have been analyzed by many authors (references 2, 18, 19 and 20 being given as examples).

The effect of the shape of the airfoils tested is not negligible; this is illustrated in Figure 17 which regroups Figures 7, 8 and 9 of reference 19.

We will note that:

- within the range of the thicknesses tested, the lower the airfoil thickness, the lower its maximum lift capabilities in unsteady flow (as well as

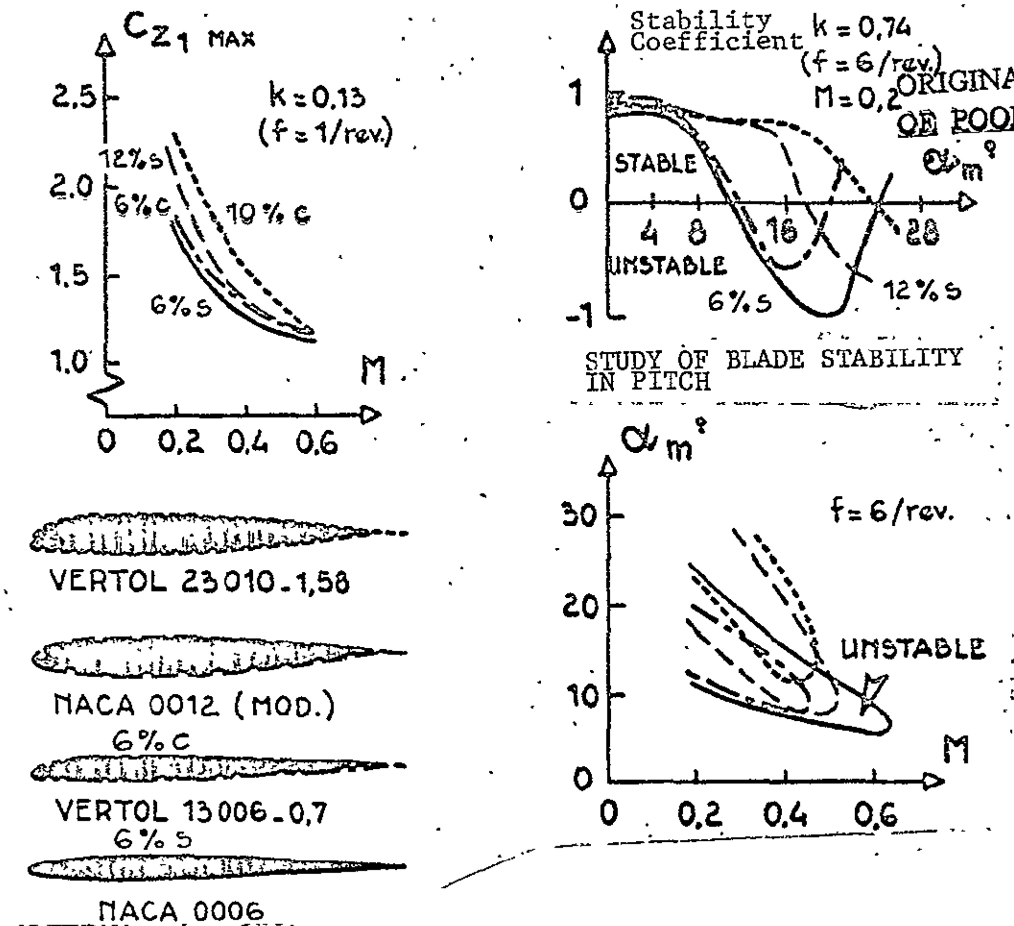

Figure 17 – Effect of the thickness and camber of the airfoil. Boeing-Vertol tests with airfoils oscillating in pitch. $\bar{\alpha} = \pm 5^{o}$

---

in steady flow). Moreover, the average incidence angle at which the airfoil becomes unstable decreases with a decrease in airfoil thickness. The instability pocket of thin airfoils extends closer to the high incident Mach numbers than is the case for thick airfoils.

– the effect of the camber is generally favorable and, as is the case in steady flow, this effect provides greater maximum lifts than are available with symmetrical airfoils with an equivalent thickness. Pitch instabilities then appear at higher average incidence angles for a fixed Mach number, or at a higher Mach number with a fixed average incidence angle.

We have been able to observe an "instability pocket" in the average incidence/Mach number plot for the test. This involved oscillations with average amplitudes (±5°). Phenomena associated with both compressibility and stall being highly non-linear, we must expect these pockets to depend on the amplitude and pitch instabilities to exist at Mach numbers greater than Mach 0.6, for example, with low-amplitude oscillations.

Figure 18 gives an axample of this and is extracted from the stall flutter test results obtained from tests conducted by the Direction des Structures (Structures Management Office) of ONERA (reference 21).

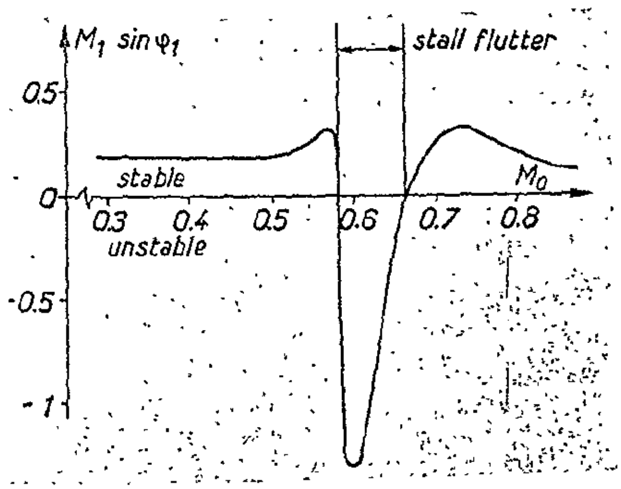

Figure 18 - Example of a result obtained in a stall flutter study. Oscillation axis located at 0.375c. NACA 63A015 oscillating in pitch - α_0=10°.

Outside of the tests already mentioned, we can obtain information on unsteady flow characteristics of other airfoils thanks to tests conducted by the RAE on the NPL 9615 airfoil for example (reference 22) or by the

Toulouse CEAT (Toulouse Aeronautical Test Center) in France using the SA 13109 airfoil for example (reference 23). New test benches designed more specifically for high Mach number tests are being assembled or are just entering into operation. These include, as examples, facilities planned at Ames and Langley Field by NASA, or at the ARA of Bedford under the RAE.

3.3. - Other motions.

If the analysis of dynamic stall phenomena was performed on changes of model incidence angles, it is because we have a lot of information available on the motion associated with these angle changes.

We note also:

- the up-and-down motions of the airfoil obtained by subjecting it to cyclical variations in translation perpendicular to the upstream flow velocity at infinity U_∞. A few typical characteristics of the tests performed by Boeing-Vertol (references 16 and 17) are provided in references 18 and 19. However, we will note that this motion is equivalent -as a first approximation- to a variation in the airfoil incidence angle with a $h\omega/U_\infty$ modulus, h being the amplitude of the up-and-down motion and ω being its pulse. Differences are caused by the fact that, over the airfoil, the distribution rule for the velocities induced by the motion is linear along the pitch oscillation motion whereas it is constant along the up-and-down motion. Figure 19 gives an example of the cycles obtained and confirms the possibility of obtaining unsteady lifts that are still greater than steady flow stall lifts but at the cost of large negative moments and of motion instabilities. Figure 20 depicts the evolution of the primary values that are characteristic of dynamic flow configurations as a funtion of the airfoil setting angle and of the upstream Mach number at infinity,
- the back-and-forth motion of the airfoil. The motion is then a cyclical translation of the airfoil in a direction parallel to the upstream air flow velocity at infinity U_ω. In fact, we obtain a cyclical modulation

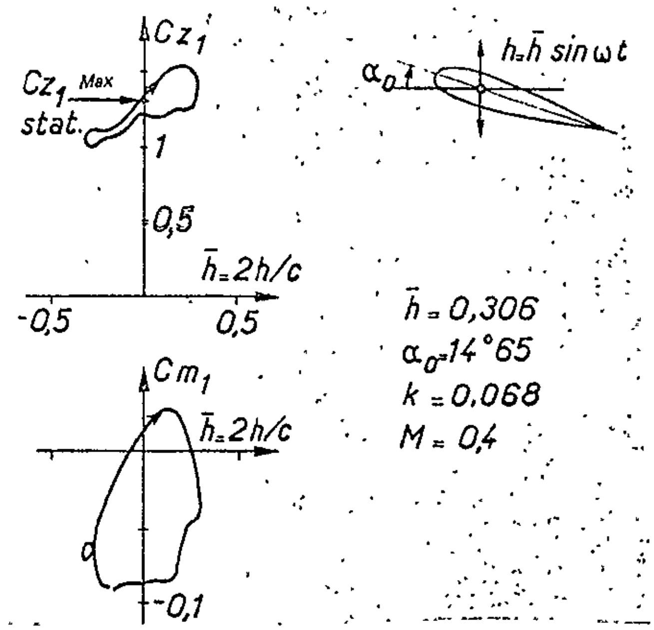

ORIGINAL PAGE IS
OF POOR QUALITY

Figure 19 - Example of unsteady cycles obtained by moving the Vertol 23010-1.58 airfoil up and down.

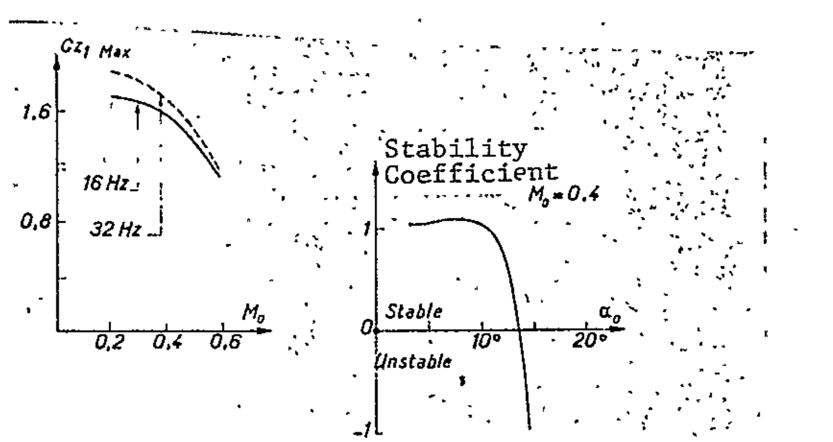

Figure 20 - Maximum lifts and Stability coefficients for the Vertol 23010 airfoil with up-and-down oscillations.

---

of the airfoil attack velocity reproducing, for example, the conditions of sinusoidal attack velocity for a helicopter blade section during a translation flight. It is the Marseille IMF that is working in this area in France (references 24 and 25). There again, there is a possibility of obtaining, during these motions, lifts that are greater than those obtained with steady flow, depending on the incidence angles to which the airfoil has been set (greater or equal to the stall indidence angle under steady flow conditions), the reduced frequency of the motion $k=\pi f\ell/U_\infty$ and of its reduced amplitude $\lambda= A\omega/U_\infty$ (A being the actual amplitude of the back-and-forth motion). Figure 21, derived from Figure 1 in Reference 26 illustrates this point but the paper presented by the Marseille IMF engineers during this meeting (reference 27) will make it possible to cover in greater detail the flows associated with this motion and the aerodynamic performances thus obtained. This attack velocity variation can also take place by varying the flow velocity inside the tunnel with the airfoil remaining fixed. This type of installation has been adopted in the United States at the University of California at Monterey, at the University of Texas and at the University of Illinois. Tests performed at the latter university using a NACA 0012 airfoil will be presented during this meeting by L.S.Saxena, A.A. Feher and M.V.Morkevin (paper #22).

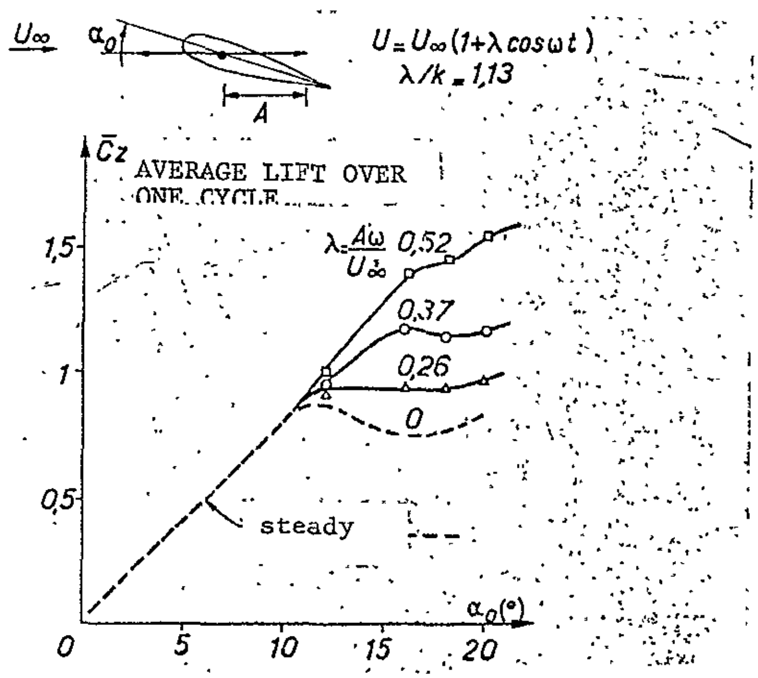

Figure 21 – Back-and-forth harmonic oscillations with a NACA 0012 airfoil. $1 < Re_c < 2x10^5$.

4 - PREDICTION METHODS

To predict the complex phenomenon that dynamic stall represents, we have different methods available. Some bring only partial information; others pertain to potential flows with or without displays of unsteady boundary layers and separations. The others, based on the solution to the Navier-Stokes equations are promising but are still in limited use. We also have available practical methods of an empirical nature when we are only interested in overall unsteady flow forces.

This paragraph will attempt to provide some information on the various available methods illustrated through several characteristic results.

4.1. - Computations of unsteady potential flows in the absence of separations.

When airfoils are not subjected to large viscous effects or separations, the solution of unsteady equations for perfect fluid mechanics makes it possible to describe in an adequate manner the pressures, forces and moments applied to the airfoils.

Basic theories apply to airfoils with zero thickness and harmonic motion. Theodorsen's theory (Figure 15), for example, reveals naturally, in its formulation, the notion of motion reduced frequency ($k=\omega c/2U_\infty$) and its effect on the modulus and phase of the pressures, forces and moments relative to the imposed motion. However, only the terms corresponding to the fundamental harmonic of ω are computed and they are proportional to the amplitude of the motion.

A simple extension of this method to the case of thick airfoils has been proposed by W.J. McCroskey (reference 28) who provides velocity distributions on top and below oscillating airfoils. Associated with the solution to the Bernoulli equation, the method shows the existence of ω terms which then depend on the shape of the airfoil (camber and thickness effect), of the average incidence angle, of the amplitude and of the reduced frequency and also of the amplitude of the 2ω terms which depend on the amplitude and reduced frequency of the motion. This method has provided good matches with test results obtained by R.I. Windsor (reference 14) and can be used to perform computations for unsteady boundary layers, for example.

The advantage of these methods is to provide a mathematical formula that is relatively simple once the Theodorsen functions are known, these functions depending on the only reduced frequency.

Geising (reference 29) has perfected a much more sophisticated computation process by applying a method making it possible to handle any type of airfoil in any type of unsteady motion. Computations can only be performed on a computer, starting with an airfoil at the rest position. At every time period, we compute the intensity of the sources positioned on the airfoil and of the associated vortices located inside the airfoil, and the position of the free vortices released from the trailing edge to form the unsteady wake, the development of which is also computed in space. Taking the Kutta-Joukowski condition into consideration, this computation makes it possible to predict the evolution of pressures, forces and moments acting on the airfoil. If a few computation procedures for unsteady flow in the absence of any separation from the airfoil have been recalled here, it is because:

- for any dynamic stall configuration, there are times when there are no separations from the airfoil,
- the analysis of the results provided by these methods can partially explain stall delay.

The Theodorsen theory shows through an example that when the incidence angles of an airfoil oscillating in pitch increase, the pressure gradients along the chord are less than the pressure gradients obtained in a steady flow. Can this observation made by F.O. Carta (reference 30) be sufficient to explain the stall delay? Figure 22, extracted from reference 1, shows the result obtained by assuming that the unsteady stall (α_{DS}) takes place only when the unsteady pressure gradient near the airfoil leading edge (at x/c=0.1) reaches the theoretical value for steady flow separation. Computations properly predict, as is actually experienced, that the unsteady stall incidence angle increases with the reduced frequency of the motion but computations are far from being able to predict the absolute value of the increase in the stall incidence angle in dynamic stall configurations.

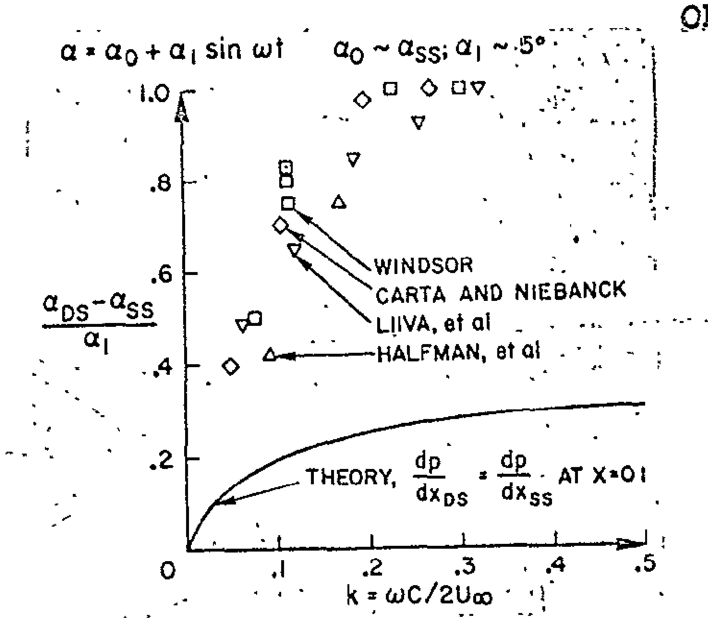

Figure 22 - Increase of the unsteady stall incidence angle α_{DS} against the steady stall incidence angle α_{SS}.

4.2. - Computations of dynamic stall configurations using potential flows.

We have seen that, experimentally, one of the major phases of stall was the formation and displacement of a vortex on the top side of the airfoils.

- Professor Ham (reference 31) has simulated this phase by generating near the leading edge a series of vortices and by letting them escape toward the trailing edge at the local flow velocity. This computation has been made for the case of an infinitely thin airfoil.

Figure 23, extracted from reference 31, shows the trajectories followed by the vortices in the case of a flat plate suddenly subjected to an incidence angle of 30^o. We can readily see a vortex mass being generated and moving toward the trailing edge.

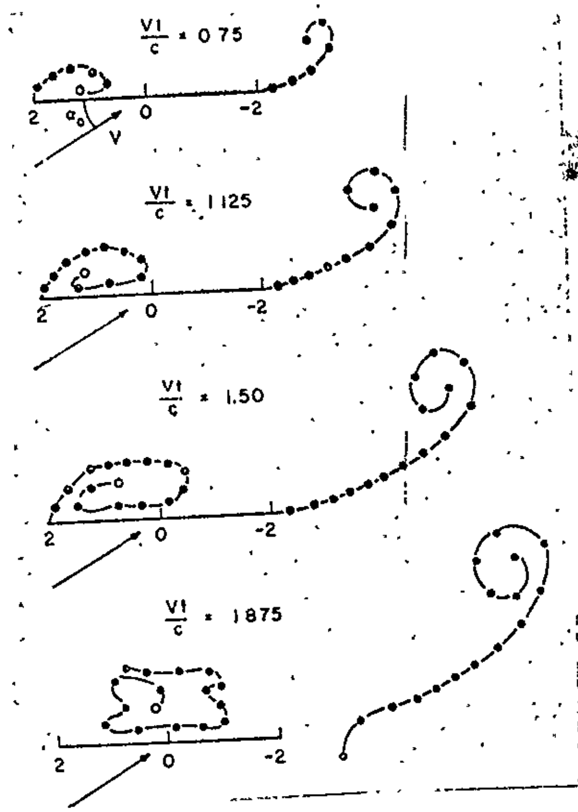

Figure 23 - Computed trajectories for the vortices generated when the incidence angle is suddenly set to 30^o.

Figure 24, also extracted from reference 31, shows a satisfactory agreement with actual experience with respect to local pressures on an airfoil oscillating in pitch between 10 and 30^o at a reduced frequency of 0.35 (tests performed at MIT).

However, it must be noted that we must assume the time at which leading edge vortices are emitted. Moreover, computations cannot take into consideration trailing edge separations.

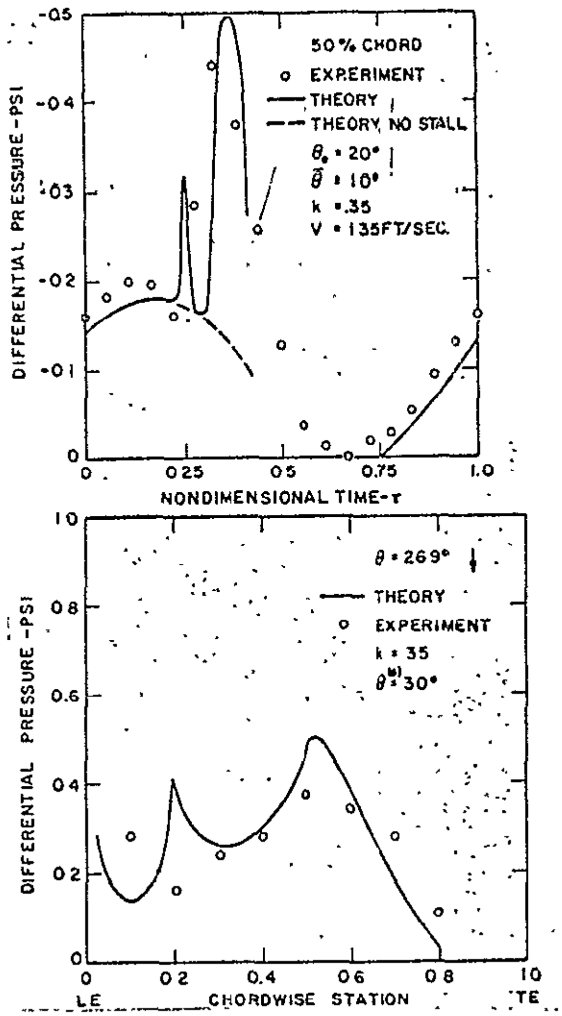

Figure 24 - Computed and experimental evolution of the pressures on an airfoil in a dynamic stall configuration.

- In France, the Société Bertin (references 32 and 33) has used this scheme by applying it to the case of an airfoil. But it is the separation of the boundary layer taking place toward the trailing edge that generates a vortex layer. This layer is generated from this point and is fed with a rotational flow by the boundary layer. According to Sarpkaya (reference 34), the rotational flow rate is given by the formula: $\Delta\gamma/\Delta t = -1/2\ (U^2-U_r^2)$.

where U is the flow velocity at a right angle to the point of laminar separation and U_r is the maximum velocity of the recirculation flow induced by the vortex winding action.

At every point in time, we therefore emit discrete vortices for which we compute the trajectory. We determine the velocities induced at the airfoil wall by all of the singularities corresponding to the J.P. Geising method (reference 29) and by the free vortices generated at the leading edge.

Figure 25, extracted from reference 33, shows a comparison between computed vortex lines and smoke visualizations performed by the Ames USAAMRDL (reference 6). Comparisons of lift cycles obtained are rather encouraging, as shown in Figure 26 extracted from reference 2.

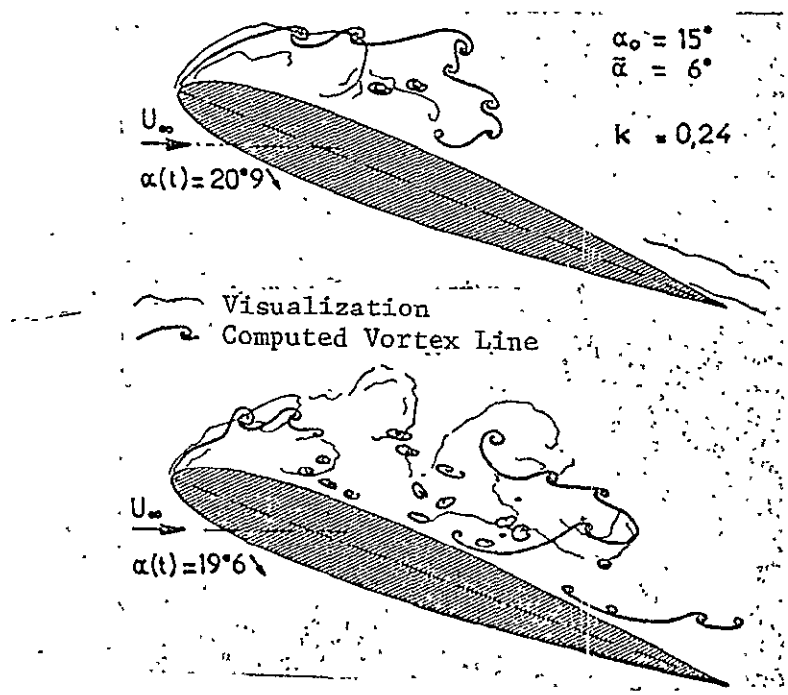

Figure 25 - Evolution of unsteady separation. Comparison of computations and visualization. $\alpha_0 = 15^\circ$; $\bar{\alpha} = 6^\circ$; $k = 0.24$.

However, there remain some problems in determining either rigorously or empirically (under study) the conditions for the generation and diffusion of these vortices.

Potential flow computations still have their own limitations and only unsteady boundary layer computations can bring information elements to make it possible to understand and possibly predict the delays in the appearance of separations.

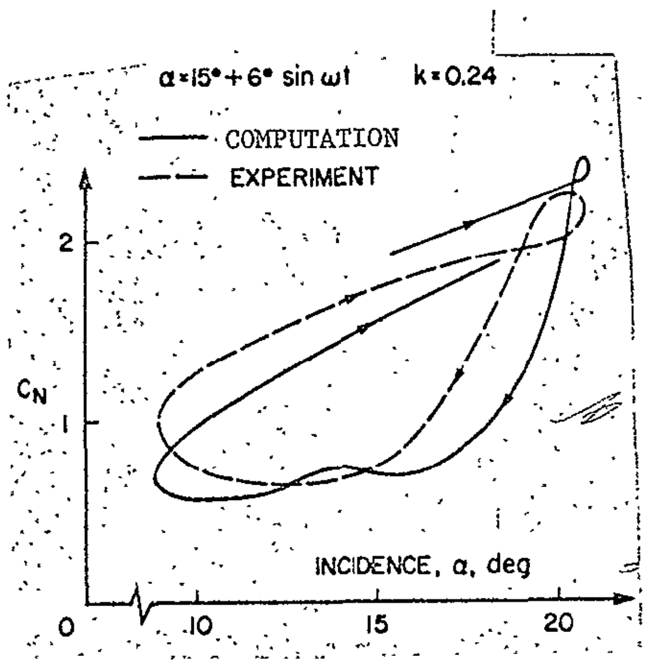

Figure 26 - Comparison of Bertin computations and USAAMRDL (Ames) tests. NACA 0012 airfoil.

4.3. - Computations of unsteady boundary layers.

One of the sessions in this unsteady aerodynamics meeting is devoted to the problems of the unsteady boundary layer, whether separated or not; it is preceded by an overall presentation by D.P. Telionis; therefore, it is not useful for us to develop this subject here.

Here, we will only recall a few fundamental problems associated with dynamic stall configurations.

Figure 27, extracted from reference 1, shows that in the case of the oscillating airfoil, the effect of the unsteady terms $\frac{\partial u}{\partial t}$ in the turbulent boundary layer equations is not negligible in the area where the drag coefficient becomes zero. In the computations that were performed, we took the velocity distribution laws for potential flow as determined by W.J. McCroskey (reference 28). The hysteresis effect which is observed to be more significant when we consider the $\frac{\partial u}{\partial t}$ terms comes primarily as the result of the fact that near the trailing edge, these time derivatives are of the same order of magnitude as the gradients along the chord $u \frac{\partial u}{\partial x}$.

ORIGINAL PAGE IS
OF POOR QUALITY

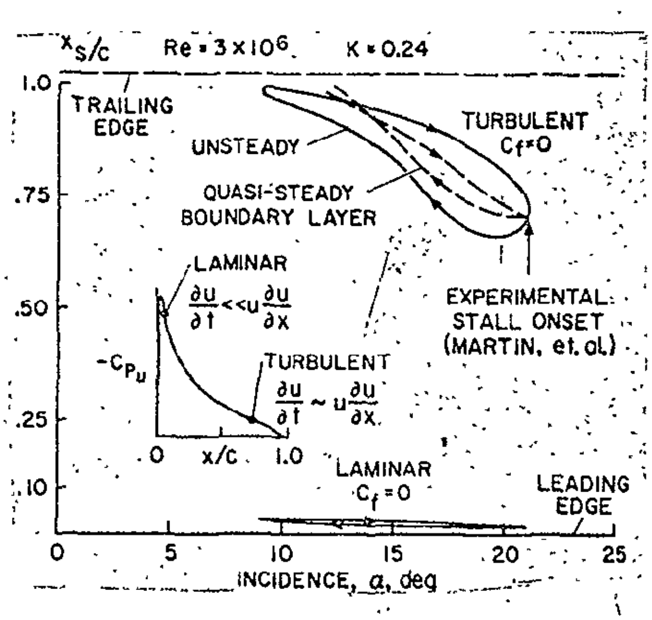

Figure 27 - Evolution of the point of zero drag coefficient with an oscillating NACA 0012 airfoil. $Re=3x10^6$; $k=0.24$; $\alpha=15^o+6^o$

A detailed analysis of the reversal toward the leading edge of the point where a reverse flow appears (equivalent to the point where the drag coefficient is zero) was performed by R.M. Scruggs, J.F. Nash and R.E. Singleton (reference 35). Figure 28, extracted from this last reference, shows the computation results obtained with an airfoil subjected to an increasing incidence angle variation performed at a constant velocity and between 0° and 25°. If we consider the computations performed with the unsteady potential flow and the unsteady boundary limit, the point where the reverse flow appears starts moving toward the leading edge later but, with an increasing incidence angle, it moves much faster than in steady flow. The delay in this motion is caused, according to the authors, in part by the unsteady potential flow and in part by unsteady boundary layers as shown in the different curves of Figure 28.

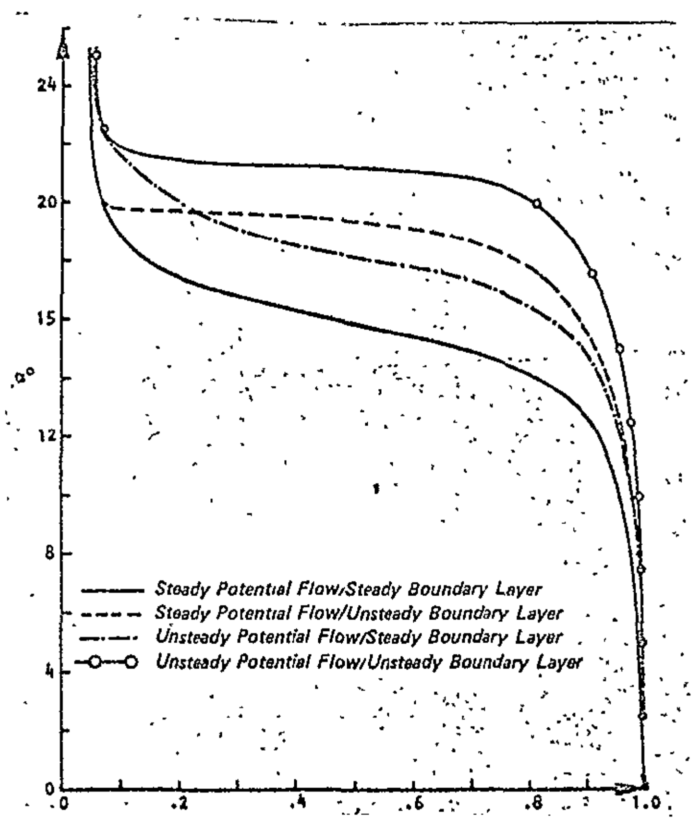

Figure 28 - Motion of the point where reverse flow appears. (Increasing incidence angle and $c\dot{\alpha}/u_\infty$=0.04)

It is significant to note (Figure 29, extracted from reference 35) that if we consider the incidence angle at which the point where reverse flow takes place appears at mid-chord, this angle will increase with the speed of airfoil angular variation in a manner very similar to lift with respect to the steady stall incidence angle. This increase is at first very steep for low values of $c\dot{\alpha}/2U_\infty$ and then there appears a type of saturation of the unsteady effects at high values of $c\dot{\alpha}/2U_\infty$. This characteristic phenomena reportedly originates also in part from the unsteady potential flow and in part from the unsteady boundary layers.

ORIGINAL PAGE IS
OF POOR QUALITY

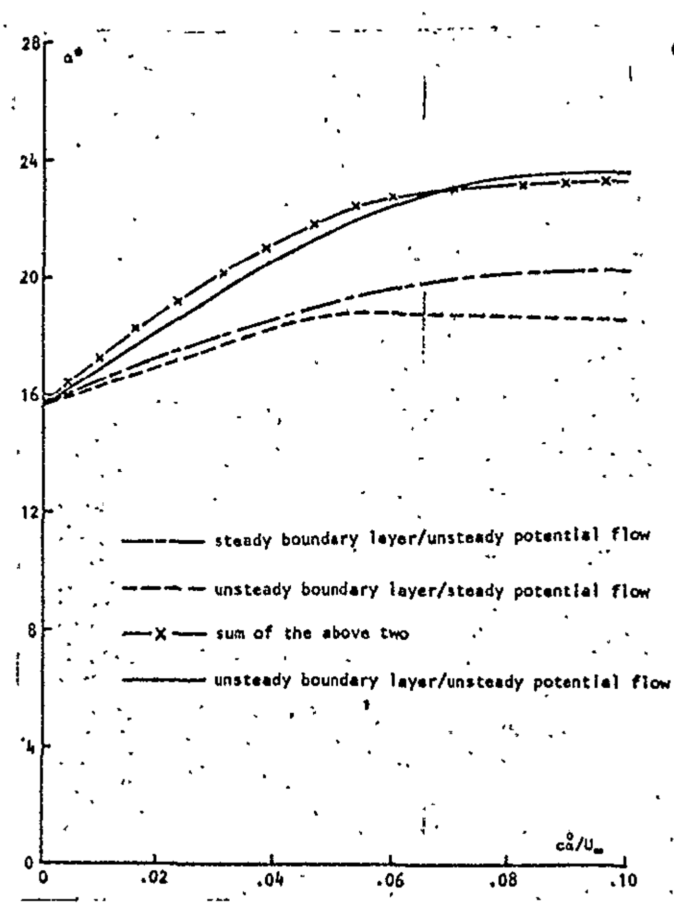

Figure 29.- Incidence angle at which reverse flow reaches the airfoil mid-chord as a function of the angular velocity of the airfoil.

However, we must state that these computations can really be meaningful only if the point where reverse flow appears is not followed downstream by too large a boundary layer separation which would then change velocity distributions over the entire airfoil (this would appear to be the case with tests performed at Ames using the NACA 0012 airfoil with or without its cambered extension).

A major point associated with the unsteady nature of boundary layers is the distinction between the point where reverse flow appears and the point of separation. Very many studies have been conducted in this subject area and the reader can refer to certain papers given as examples:

- papers presented at the IUTAM Symposium on unsteady boundary layers organized by Laval University, Quebec, Canada, in May 1971 (reference 36),
- papers presented at the symposium organized by the University of Arizona, Tucson, in March 1975 (reference 37), on unsteady aerodynamics.

In fact there does not appear to be any singularity at the point of reversed flow as in stationary flow. For example, the separation criterion is involved only upon the appearance of the divergence of the displacement thickness. This takes place upstream from the point where reversed flow appears as shown in the sketch of figure 30 proposed by W.R. Sears and D.P. Telionis (reference 38). Therefore, we can continue to describe the boundary layer upstream of the point of reversed flow ($c_f=0$). V.C. Patel and J.F. Nash were able to compute (reference 39) the change in time of a turbulent separation bubble created by a deceleration followed by an acceleration of the external flow which is variable in time. Figure 31, extracted from reference 2, illustrates the results obtained which show the birth of the separation bubble with its reversed flow, its extension toward the leading edge and the final appearance of separation caused by the sudden increase of the boundary layer thickness. These phenomena of unsteady turbulent separation bubbles are also studied in an intensive manner by L.W. Carr of the Ames USAAMRDL.

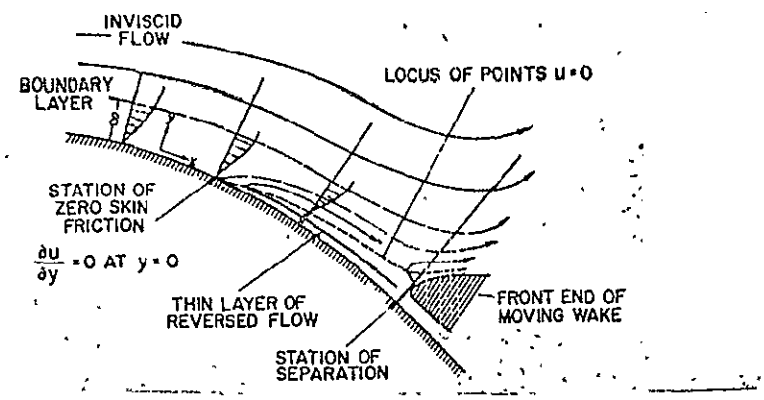

Figure 30 - Sears and Telionis model for the separation of a boundary layer moving back toward the leading edge.

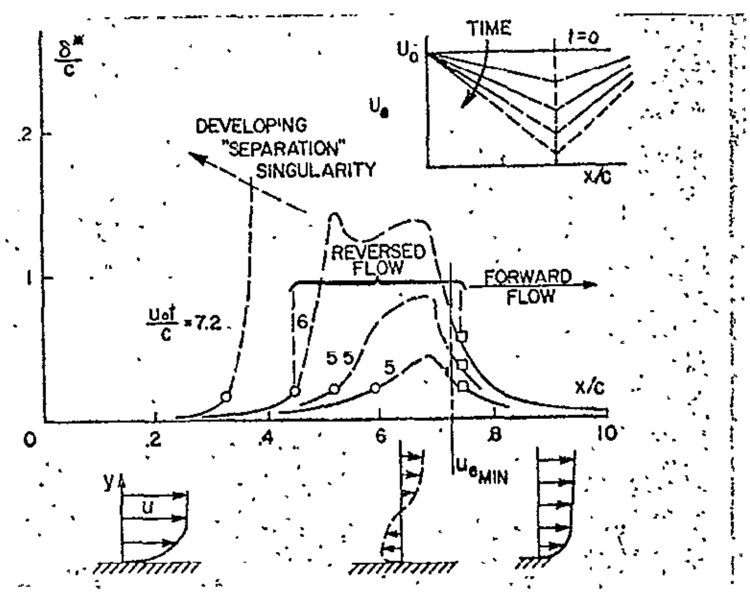

Figure 31 - Computation of the variation in the displacement thickness of an unsteady turbulent boundary layer with reversed flows.

There are many methods for computing unsteady turbulent boundary layers but we must mention that the selected turbulence models are, for the time being, always based on criteria that are valid for steady flow. It would therefore appear fundamental to this field to check that these models are suitable to unsteady aerodynamics. Experiments based on research of unsteady boundary layer characteristics will therefore be very useful and we will mention, as an example, the work performed by the Toulouse CERT-ONERA with flat plates subjected to pulsed flows. This work will be the subject of a presentation during session III of this meeting (reference 40).

In conclusion, boundary layer and potential flow computations provide interesting partial data and make it possible to understand certain phases of unsteady stall. However, they remain incomplete.

4.4. - Navier-Stokes Equations Computations.

In a problem as complex as the interaction between potential and viscous flows, the solution of the Navier-Stokes equations should make it possible to approach the dynamic stall problem in its entirety.

In solving the vortex propagation equation and Poisson's equation for the stream function through a scheme using finite differences and a relaxation procedure, U.B. Mehta and Z. Laven had already used the stall of an airfoil after it had suddenly been set to an angle of attack (reference 41). A similar approach was used for the case of an oscillating airfoil and U.B. Mehta will present, during this symposium, the results that he has obtained (reference 42). Visualizations obtained at the ONERA aerodynamic tunnel under conditions corresponding to those used in the computations make it possible to determine the accuracy of the preliminary results obtained. Figure 32 shows a very good agreement between the computed streamlines and the paths of the air bubbles used to make visualizations possible. The vortex phenomena are properly predicted and we can therefore hope that computations will be able to describe in a satisfactory manner the physical process involving the birth, convection and eventual dissipation of these vortices which are characteristic of unsteady flow.

It is hoped that computations can be made with more realistic Reynolds numbers by using turbulence models that are suitable to cases involving strong viscous interactions.

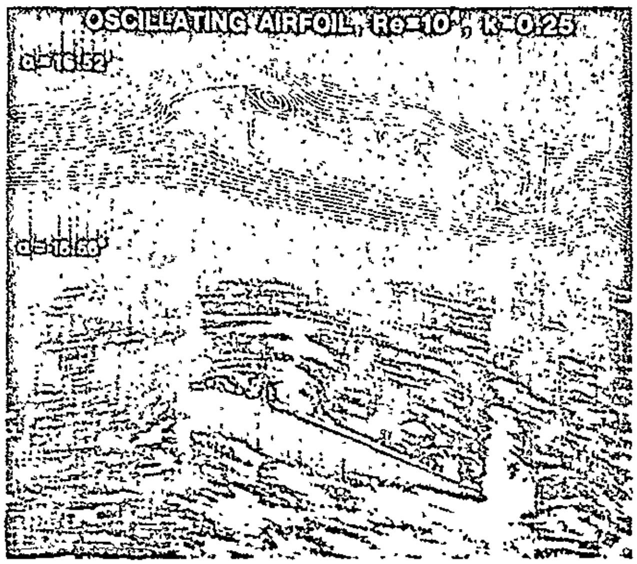

Figure 32 - NACA 0012 oscillating in pitch.
$\alpha = 10^{\circ} + 10^{\circ} \sin \omega t$; $k=0.25$; $RE_C = 10,000$

During this meeting, other papers also cover the solution of the Navier-Stokes equations. The paper by J.C. Wu and N.L. Sankar also involve an oscillating wing (reference 43) and the paper by R.B. Kinney covers the case of a fixed wing subjected to unsteady flows (reference 44). The methods used to solve the Navier-Stokes equations may be different and it will be interesting to learn if some methods can be applied to higher Reynolds numbers without requiring prohibitive computation times.

Another application of the Navier-Stokes equations was made by S.J. Shamroth and J.P. Kreskowsky (reference 45) by using them only near the leading edge. Computations provide a rather detailed description of the leading edge laminar separations and could therefore be used for leading edge dynamic stalls through, for example, the bursting of separation bubbles.

4.5. - Problems caused by the coupling between viscous and inviscid flow.

We can also use the so-called coupling methods which make it possible to compute pressure distributions by performing perfect fluid computations taking into consideration the development of viscous layers through the use of conditions at the limits.

Figure 33 illustrates a trailing edge turbulent separation configuration with reversal toward the airfoil leading edge. In one coupling method, it will be necessary to take into account the laminar boundary layers, the transition, the turbulent boundary layers, the separation areas and the wake.

For example, to take the boundary layer into account different methods already applied to stationary flow are possible:
- we can redo potential flow computations after enlarging the airfoil with the computed displacement thickness using a boundary layer program and then iterating until there is convergence;
- we could also distribute along the airfoil a series of sources and "wells" corresponding to the flow rate variation affected by the boundary layer; the intensity of these singularities ($q=d/ds(\rho_e U_e \delta^*)$) is computed from computation results for viscous and potential flows in the preceding iteration.

The transition takes place in many cases by means of a laminar separation bubble. Unsteady conditions to which the airfoil may be exposed can retard its bursting. Work performed by J.D. Lang (reference 46) is, for example, interesting in this regard. The purpose of this separation bubble can certainly become important in the case of airfoils which, in steady flow, stall through this bubble bursting. We must also mention

ORIGINAL PAGE IS
OF POOR QUALITY

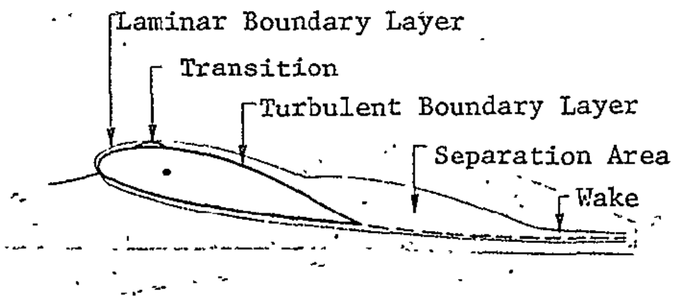

Figure 33 - Example of viscous areas over an airfoil in a dynamic stall configuration.

the studies in this area performed at MIT by N.D. Ham and his team (references 72, 73, and 76).

The problem of the separation area and of the wake remains much more complex and deserves in-depth study. We can mention the studies by P. Crimi (references 47 and 48) who, in his work for predicting forces and moments on airfoil in a dynamic stall configuration, makes the hypothesis, for example, of a constant pressure in the separation bubble.

The separation point on the airfoil is assumed to be known but is redefined at every consecutive iteration between computations of the viscous and potential flows until there is convergence at that point.

By assigning a law for the displacement of the separation point on an oscillating airfoil, F. Sisto and P.V.K. Perumal (reference 49) have computed the evolution of the forces and moments. For potential flow computations, they used a potential acceleration method. Computations made for a flat plate oscillating in pitch and moving in a pumping action show that we can thus obtain force and moment cycles that can lead to flutter. In fact, the selection of singularities to depict separation areas and the viscous wake coming from the merging of the boundary layers on the upper and lower surfaces seems to demand further in-depth analyses.

Nevertheless, the theoretical aspect of this problem has been recently examined by W.R. Sears (reference 50) who covers in particular the delicate problem of the Kutta-Joukowski condition in unsteady flow.

It would perhaps be interesting to develop methods similar to those developed for predicting the maximum lift of airfoils in steady flow as B. Maskew and F.A. Dvorak (reference 51) have just done.

The problem of coupling between viscous and inviscid flows will certainly require much effort but the goal to reach is most attractive since it should provide a much more accurate computation of dynamic stall configurations and of the aerodynamic qualities of the airfoils under these conditions.

4.6. - Empirical Methods for Predicting Overall Forces.

The preceding paragraphs show the different fundamental problems that have to be resolved to describe in an accurate manner the various phases of dynamic stall. For years, with a goal of using them for applications, many researchers have devoted themselves to finding simpler methods for representing unsteady forces with airfoils encountering dynamic stall regimes during unsteady motions.

The problem consists primarily of finding a very general formula from tests performed with simple configurations (oscillating airfoil, for example) while varying many parameters: airfoil, Mach Number, incidence angle and amplitude, etc..

UARL Method (α, A, and B).

This method has been perfected by F.O. Carta and rests on the fact that instantaneous lift and pitching moment must be functions -as in non-separated unsteady flow- of the incidence angle α, of the angular speed $\dot{\alpha}$ and of the angular acceleration $\ddot{\alpha}$.

In fact, Carta uses, for greater generality, the following reduced parameters: $\sigma=\alpha/\alpha_{DS}$; $A=\dot{\alpha}c/2U_\infty$; $B=\ddot{\alpha}c^2/4U_\infty^2$ where α_{DS}=steady stall incidence ang.

ORIGINAL PAGE IS OF POOR QUALITY

We have tables available (references 52 and 53) which provide for any incidence angle average C_z or C_m values for corresponding A and B values.

This method has made it possible to resolve many problems associated with dynamic stall configurations or with configurations where aerodynamic instabilities appear (flutter) on a compressor or helicopter rotor (references 54 through 56).

More recently, R.L. Bielawa from the United Technologies Research Center in Hartford (reference 57) has developed a method that makes it possible to break away from tables using A and B values. Non-linear functions for which only the coefficients are tabulated synthesize the C_z (or C_m) curves = $f(\alpha, A, B)$.

These methods can , for example, be applied to determine the angles of attack assumed by a model totally flexible in torsion when subjected to forced oscillations in pitch. Figure 34, extracted from reference 57, shows the good match that exists between experiments and computation results.

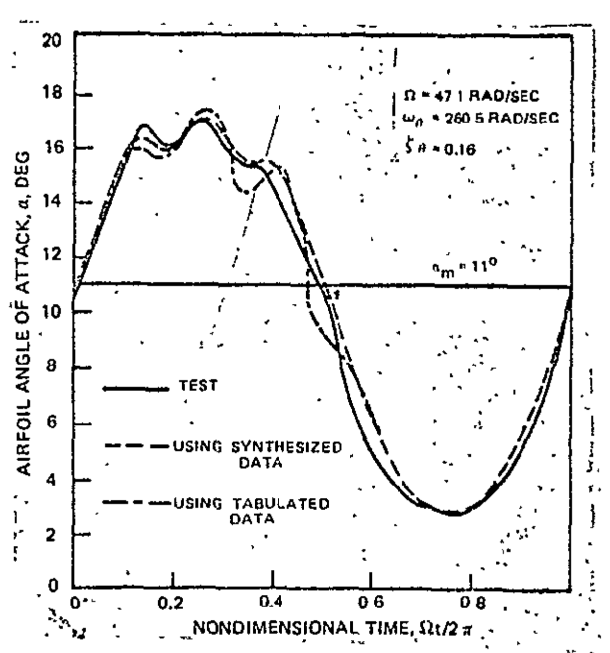

Figure 34 - Comparison of the incidence angles assumed by a flexible model subjected to forced oscillations in pitch (ω_θ/Ω=5.53).

Boeing-Vertol Method.

This method was developed following a test program with airfoils oscillating in pitch and moving in a pumping motion performed by Boeing-Vertol (references 16 and 17). It rests on the experimentally observed fact that unsteady effects are generally greater with an increase in the speed in the incidence angle variation imposed on the airfoil. D.W. Gross and F.D. Harris (reference 58) have shown that the stall delay is proportional to $\sqrt{c\dot{\alpha}/2U_\infty}$. F.D. Harris and F.J. Tarzanin (references 59 and 60) then perfected a computation of aerodynamic forces by associating with the basic theory of Theodorsen a pseudo-dynamic or unsteady reference incidence angle which indicates the possibility of having stall delay with an increasing incidence angle.

R.E. Gormont (reference 61) has described in a very complete manner the Boeing-Vertol method which has the advantage, although based on a certain amount of empiricism, of a mathematical formulation which requires only that the airfoil steady poles be known.

Figure 35, extracted from reference 60, shows that computations make it possible to predict with some accuracy the cycles of forces and pitching moments for some airfoils in the absence or presence of total or partial stall.

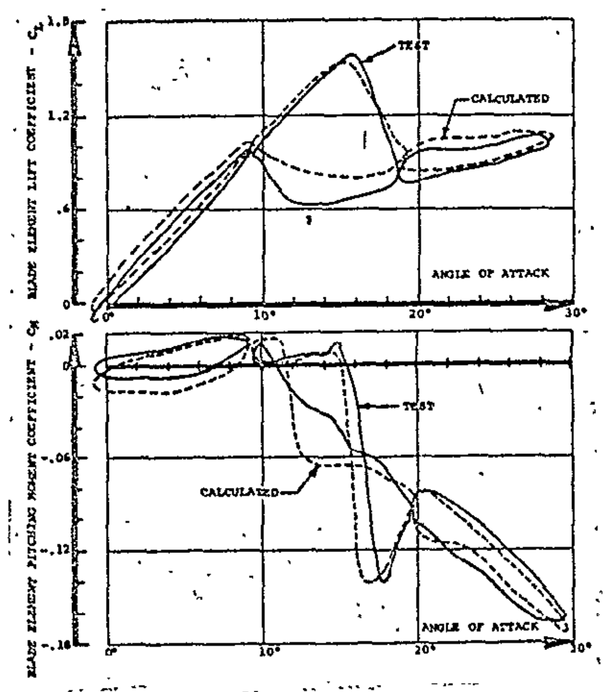

Figure 35 - Cycles of calculated and measured unsteady forces.
(Vertol 23010 airfoil- M=o.4; k=0.062)

At ONERA, this method has been modified to provide the capability to include in a program for computing local and overall performances of a helicopter rotor, the non-linear effects of unsteady stall configurations (reference 62). Figure 36 shows that a more satisfactory agreement with changes in experimental local lifts has been obtained by using this method (in comparison with the purely linear original method) on a rotor where a good portion of the retreating blade is in a dynamic stall condition.

Dynamic Stall Time-Delay Method.

This method is based on the simple idea that there could be two reduced time values τ_1 and τ_2 which determine the delay in moment stall and in lift stall. If t_0 is the original time, at the time where the airfoil has an instantaneous incidence angle equal to the incidence angle where it stalls in steady flow, the times t_1 and t_2 at which, under unsteady conditions, the airfoil stalls in moment and in lift, correspond to reduced times:

$$\tau_1=(t_1-t_2) \times \frac{U_\infty}{c} \qquad \tau_2=(t_2-t_0) \times \frac{U_\infty}{c}$$

where τ_1 and τ_2 are "universal" constants.

To Sikorsky (reference 63) τ_1 and τ_2 have values of 2 and 6; to Westland (reference 64), τ_1 and τ_2 have values of 2.44 and 5.41 after a detailed examination of the Boeing-Vertol tests (references 16 and 17) for which these average values would be valid in more than 120 configurations. From this somewhat surprising result has come a simple method of computing unsteady aerodynamic forces in the case of dynamic stall. The four primary computation phases are illustrated in Figure 37, page 46.

)As long as the airfoil does not reach the incidence angle corresponding to unsteady moment stall, computations are made in potential flow without separation.

2) For intermediate times between moment stall and lift stall, we continue to compute lifts for non-separated flows but the moment is computed by applying a linear law as a function of the recoil time of the aerodynamic locus until we have a location equivalent to that obtained in totally separated steady flow.

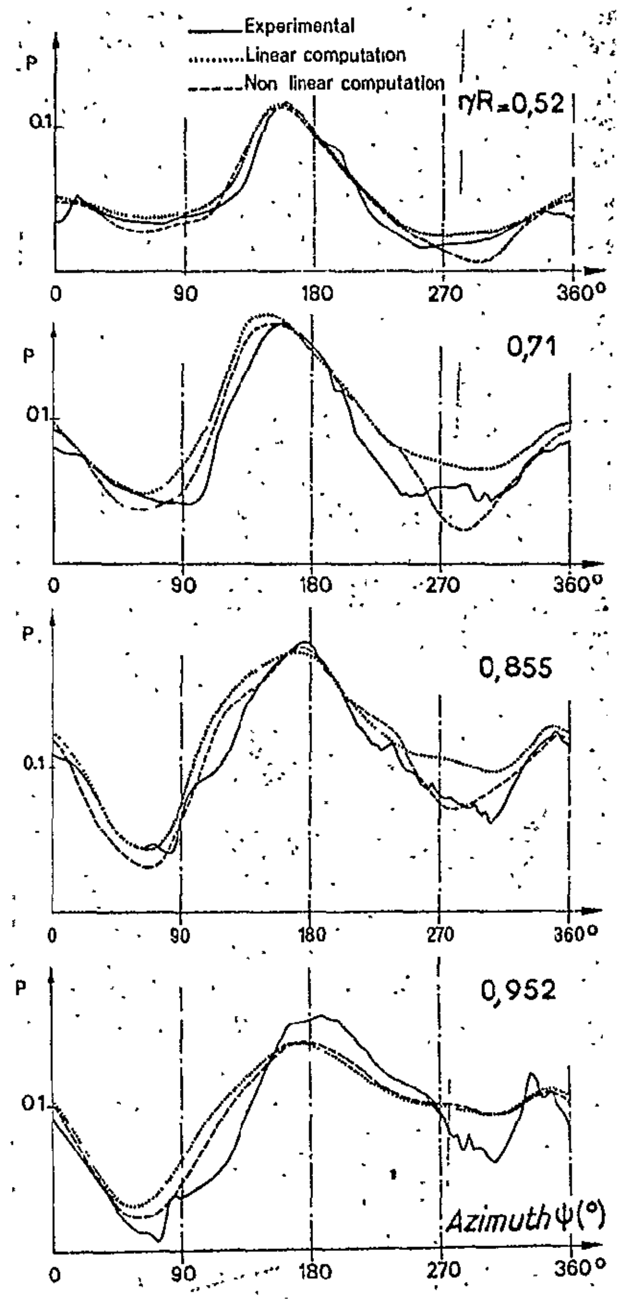

Figure 36-Evolution of local loads on a three-blade rotor under heavy load.

3) when unsteady lift stall comes into play, we apply an exponentially-decreasing law of this lift as a function of time toward values for a quasi-steady pole of separated flow over an airfoil.

4) finally, when the incidence angle once again becomes equal to or less than the steady stall incidence angle, we return to the steady poles through a re-attachment process which is also expressed mathematically.

With this method, we are also able to satisfactorily reproduce experimental lift and pitching moment cycles on airfoils in a stall configuration as shown in Figure 38 which has been extracted from works by T.S. Beddoes (reference 64). However, as in the case of the preceding methods, the agreement is not always good.

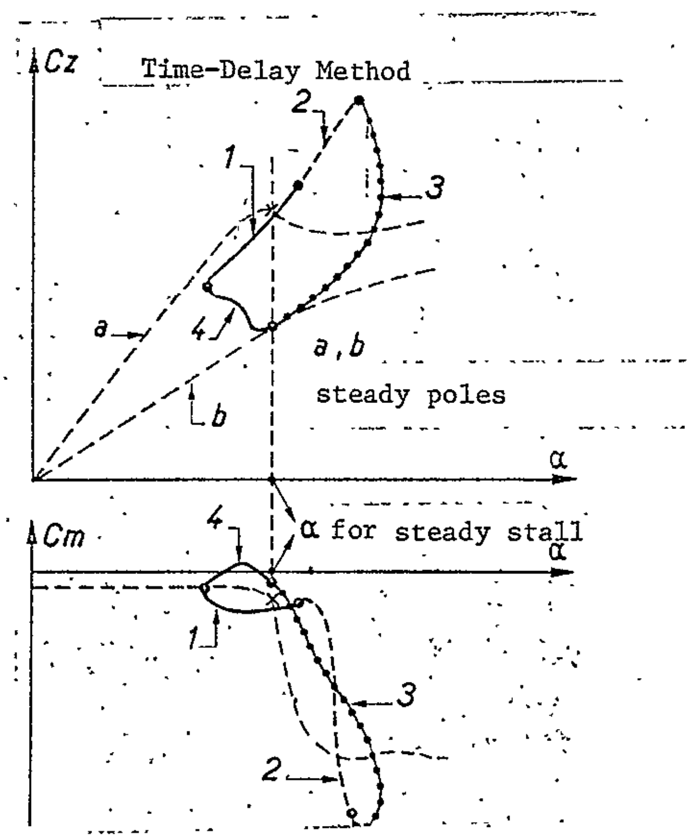

Figure 37 - Primary phases of computations performed using the "Time-Delay" method.

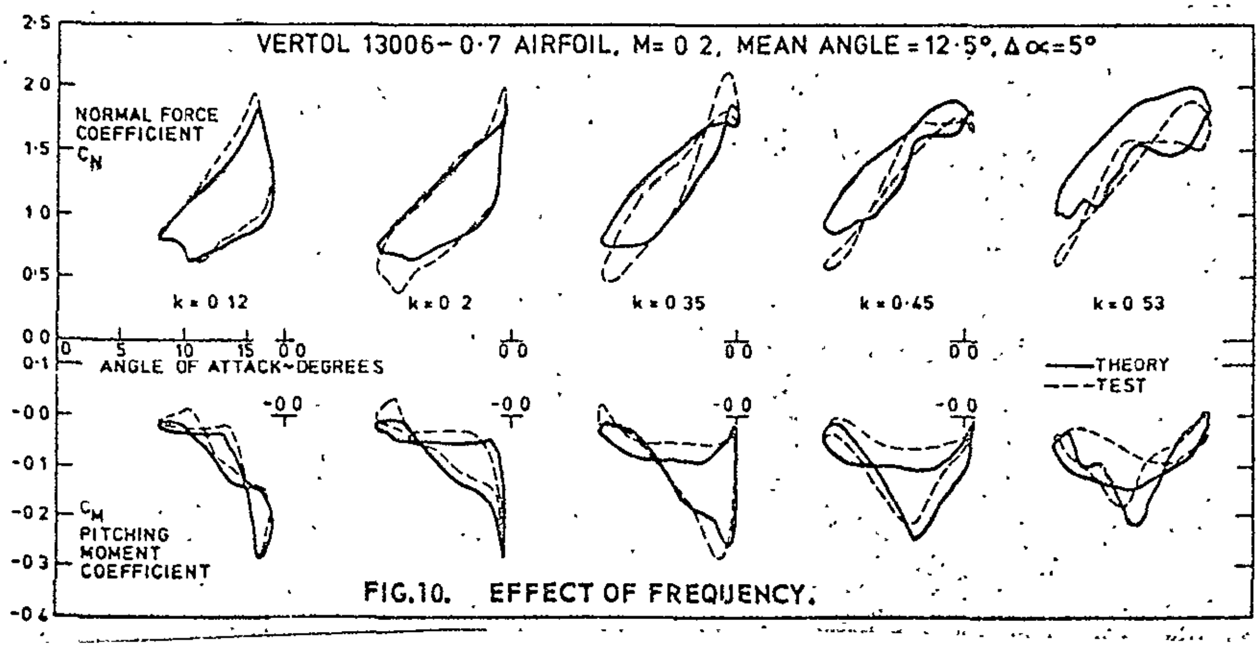

Figure 38 - Effect of the reduced frequency of harmonic oscillations in pitch on the Vertol 13006 airfoil (M=0.2; α_0=12.5°; α_1=5°)

Lockeed Method.

L.E. Ericsson and J.P. Reding base their analyses of the results and their prediction method on a half-theoretical, half-empirical decomposition of the stall delay.

Associated mathematical formulas are developed in reference 65. Their application to the case of the tests performed at Ames by the USAAMRDL sometimes gives good results as shown in Figure 39 extracted from reference 66. The phase for the appearance of moment stall is well predicted. The phase for lift stall and the phase for the appearance of the maximum negative moment are associated with a vortex propagation speed of $0.55U_\infty$ and to its passage over the 70% point on the chord or over the airfoil trailing edge.

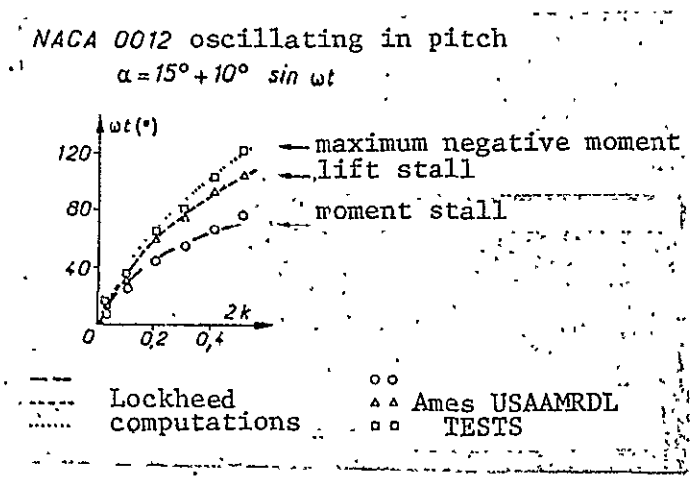

ORIGINAL PAGE IS OF POOR QUALITY

Figure 39 - Predictions of events associated with the dynamic stall of oscillating airfoils.. NACA 0012 airfoil oscillating in pitch. $\alpha=15^{o}+10^{o}\sin\omega t$.

The methods developed by L.E. Ericksson and J.P. Reding have been the subject of many documents (references 67 through 70) bearing in particular on unsteady stall, flutter or dynamic effects associated with separation behind shock waves. During this meeting, these authors present a paper (reference 71) which states the problem of scaling up the results acquired in wind tunnels which must be transposed to full-scale aircraft within the scope of dynamic tests where the Reynolds number plays a very significant role.

MIT Method.

It is based on the knowledge acquired at MIT by Professor Ham and his team in both the experimental and theoretical areas (references 72 and 73). W. Johnsson (references 74 and 75) has shown that the maximum lift and the maximum pitching moment are linearly related to the angular speed parameter $c\dot{\alpha}/2U_\infty$ but that there limiting values to their increase. The unsteady stall angle is estimated through semi-empirical formulas established by W. Johnsson and N.D. Ham (reference 76). As an example, reference 75 provides the results obtained with this method and the ones developed at Boeing-Vertol and UARL in determining local loads in a helicopter rotor.

W.J. McCroskey has provided, in reference 1, the results obtained with the various prediction methods mentioned above for determining maximum negative moments and lifts reached with the NACA 0012 airfoil tested at Ames with harmonic oscillations in pitch. Since the originial publication in March 1975, computations have been continued, particularly by Lockheed and MIT following improvements that they were able to make to their methods. Current results of the comparison between computations and experiments are provided in Figure 40. Overall, the results seem highly satisfactory but these are very partial results. It certainly would be interesting to make a more complete comparison of the various methods by looking also at the phases during which the main effects on lift cycles and particularly the moment cycle take place.

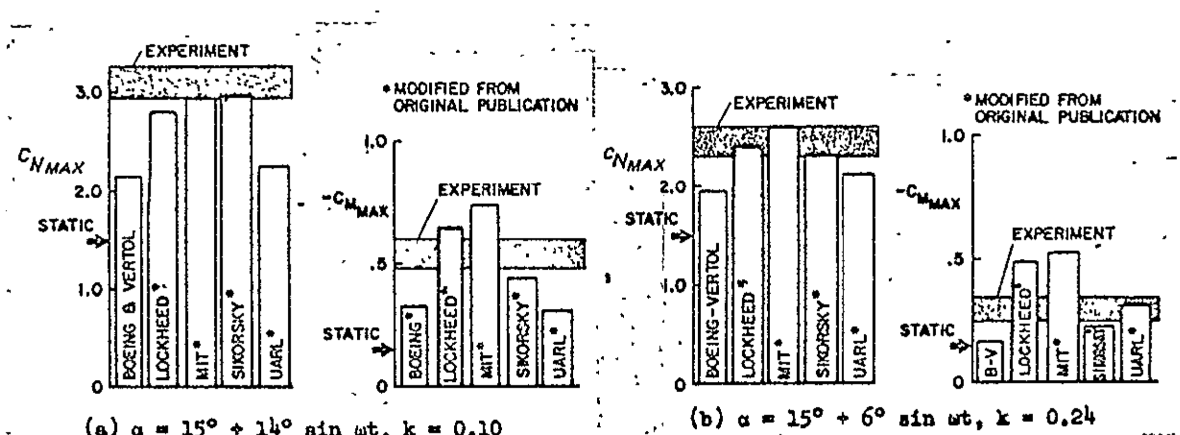

Figure 40 - Comparison of computations and experiments for normal forces and maximum negative moments reached with a NACA 0012 airfoil oscillating in pitch.

These various methods satisfy specific needs of manufacturers and researchers. The applications primarily involve helicopter rotors with certain flight configurations that impose stall conditions on the retreating blade. Dynamic loads, stresses and deformations induced by the blade stalling are clearly much better predicted by using the preceding methods than was the case a few years ago. However, there still remain significant local or instantaneous differences which justify pursuing the search for new prediction methods that are increasingly sophisticated, or for unsteady tests with a three-dimensional effect. Figure 41, extracted from reference 77, shows the test results recently obtained at Hartford with swept oscillating airfoils and the significant differences obtained with a 30° and a 0° sweep angle, with respect to aerodynamic moment cycles. It appears that this wing sweep angle increases the tendency for the airfoil to be unstable in pitch. This illustrates the aerodynamic complexity that stall configurations must have in three-dimensional and unsteady flows.

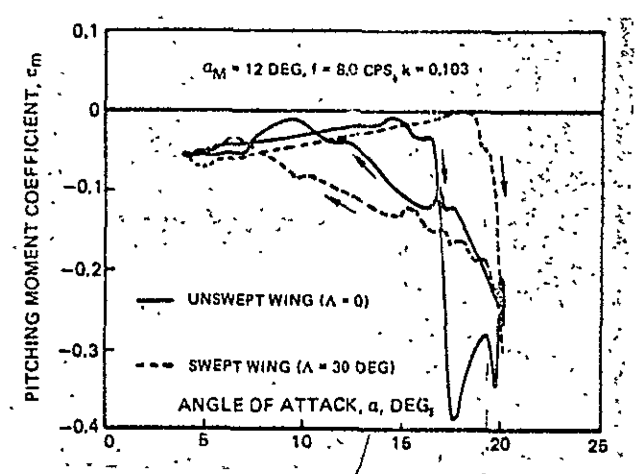

Figure 41 - Effect of a 30° sweep angle on pitching moments

5 - CONCLUSIONS

Dynamic stall is a complex example of strong interaction between viscous and inviscid flows. Even in the simple case of oscillating airfoils, experiments involving very complete measuring and observation equipment are needed order to be able to properly interpret the complex phenomena associated with such configurations. The physical process for forming and feeding vortices on top of the wing still remains poorly defined, hence difficult to show through computations. Means for predicting the evolution of unsteady forces and moments need to be perfected further. Although more or less empirical formulas are at times satisfactory, it will be necessary to have programs for the coupling between viscous and inviscid flows which take into consideration the boundary layers, separations, the wake and the vortex phenomena that are characteristic of dynamic stall.

Instabilities or flutters are one of the most important consequences of dynamic stall. Unsteady bench tests operating in transsonic wind tunnels will make it possible to have tests that are necessary to the proper understanding of the effect of shocks and separations on these phenomena.

The three-dimensional aspects of dynamic stall configurations still remain a subject that is hardly covered in detail; it is indispensable to at least insure that the transposition of the results obtained in two-dimensional flow is sufficiently accurate for resolving practical problems facing manufacturers.

In this paper, only some aspects of dynamic stall could be touched upon for reasons of clarity of presention but it is certain that other interesting works could be mentioned.

Moreover, papers that will be presented during this congress on unsteady aerodynamics will bring new results and new elements for consideration which will undoubtedly result in furthering the understanding and prediction of phenomena associated with dynamic stall configurations.

REFERENCES

[1] W.J. McCROSKEY
Recent Developments in Dynamic Stall
Symposium on Unsteady Aerodynamics
Tucson, March 1975 (published in "Unsteady Aerodynamics" Vol. 1 - Kinney R.B.
University of Arizona, July 1975).

[2] W.J. McCROSKEY
Some Current Research in Unsteady Fluid Dynamics
The 1976 Freeman Scholar Lecture.
Journal of Fluids Engineering, Vol. 99, March 1977.

[3] H. WERLE - M. GALLON
Planar flow around a model with a periodic motion - ONERA Note #239 1971

[4] J. OLSEN - H.T. LIU
The construction and operation of a water tunnel in application to flow visualization studies of an oscillating airfoil.
Flow Res. Rep. n° 13 - NASA CR 114696 (May 1973)

[5] K.W. McALISTER - L.W. CARR
Water tunnel research
NASA Report to be published in Summer 77.

[6] J.M. MARTIN, R.W. EMPEY, W.J. McCROSKEY F.X. CARADONNA
An Experimental Analysis of Dynamic Stall on an Oscillating Airfoil
J. of AHS - Vol. 19 - N° 1 - January 1974

[7] W.J. McCROSKEY - L.W. CARR, K.W McALISTER
Dynamic Stall Experiments on Oscillating Airfoils
AIAA Journal, Vol. 14, N° 1, January 1976

[8] W.J. McCROSKEY - E.J. DURBIN
Flow Angle and Shear Stress Measurements, Using Heated Films and Wires.
ASME Transactions : Journal of Basic Engineering - Vol. 94 n° 1 - March 1972

[9] W.J. McCROSKEY - J.J. PHILIPPE
Unsteady Viscous Flow on Oscillating Airfoils
AIAA Journal, Vol. 13 n° 1, January 1975 (also AIAA Paper 74-182)

10] L.W. CARR - K.W. Mc ALISTER - W.J. McCROSKEY
Analysis of the Development of Dynamic Stall Based on Oscillating Airfoil Experiments.
NASA TND - 8382 - January 1977

11] K.W. McALISTER, L.W. CARR, W.J. McCROSKEY
Dynamic Stall Experiments on the NACA 0012 Airfoil
NASA TN, to be published in 1977

[12] F.O. CARTA
Chordwise Propagation of Dynamic Stall Cells on an Oscillating Airfoil
AIAA Paper n° 75-25, January 1975

[13] A.G. PARKER
Force and Pressure Measurements on an Airfoil Oscillating Through Stall
Final Report Part II - NASA CR 145877 - August 1975

[14] R.I. WINDSOR
Measurements of Aerodynamic Forces on an Oscillating Airfoil
US Army AVLABS TR 69-98 March 1970

[15] Th. THEODORSEN
General Theory of Aerodynamic Instability and the Mecanisms of Flutter.
NASA TR 496 - 1940

[16] J. LIIVA - F.J. DAVENPORT - L. GRAY I.C. WALTON
Two-Dimensional Tests of Airfoils Oscillating Near Stall
US Army AVLABS TR 68-13, 1968

[17] L. GRAY - J. LIIVA - F.J. DAVENPORT
Wind-Tunnel Tests of Thin Airfoils Oscillating Near Stall
US Army AVLABS TR 68-89, 1969

[18] J. LIIVA
Unsteady aerodynamic and stall effects on helicopter rotor blade airfoil sections
6th Aerospace Sciences meeting - AIAA
New-York - January 1968

[19] J. LIIVA - F.J. DAVENPORT
Dynamic Stall of Airfoil Sections for High-Speed Rotors
24th Annual National Forum - AHS - Washington - May 1968

[20] J.J. PHILIPPE
Unsteady Stall of an Airfoil
Aéronautique et Astronautique n° 27, 1971-3.

[21] E. SZECHENYI
Experimental studies of dynamic forces on fixed and vibrating two dimensional airfoils
3rd European Rotorcraft and Powered Lift Aircraft Forum
Aix en Provence - Septembre 1977. To be published in "La Recherche Aerospatiale"

[22] A.W. MOORE - N.C. LAMBOURNE - L. WOODGATE
Comparison between dynamic stability boundaries for NPL 9615 and NACA 0012 aerofoils pitching about the quarter-chord.
ARC - CP 1279 - 1974

[23] J. RENAUD - F. NIBELLE
Effects of the Airfoil Choice on Rotor Aerodynamic Behaviour in Forward Flight
Second European Rotorcraft and Powered Lift Aircraft Forum. Bückeburg - West Germany - Septembre 1976

[24] J. VALENSI, J. REBONT, J. RENAUD, G. VINGUT
Aerodynamics Effects on a Wing Airfoil with harmonic motion parallel to the flow.
AGARD CP n° 111 "Aerodynamics of Rotary wings" 1973.

[25] C. MARESCA, J. REBONT, J. VALENSI
Separation and reattachment of the boundary layer on a symmetrical aerofoil oscillating at fixed incidence in a steady flow.
Symposium on "Unsteady Aerodynamics" - University of Tucson - Arizona - March 1975

[26] C. MARESCA - J. REBONT - J. VALENSI
Aerodynamic Characteristics of a Wing Airfoil with Unsteady Motion
14ème International Congress of Theoretical and Applied Mechanics - Delft - Septembre 1976

[27] J. REBONT, C. MARESCA, D. FAVIER, J. VALENSI
Dynamic reattachment on an aerofoil performing oscillations parallel to the undisturbed stream
FDP AGARD meeting on "Unsteady Aerodynamics" Ottawa - September 77

[28] W.J. McCROSKEY
Inviscid flow field of an oscillating airfoil
AIAA Journal - Vol. 11 n° 8 (August 1973)

[29] J.P. GIESING
Non linear two-dimensional unsteady potential flow with lift
Journal of Aircraft - Vol. 5 n° 2 - March-April 1968

[30] F.O. CARTA
Effect of unsteady pressure gradient reduction on dynamic stall delay
Journal of Aircraft - Vol. 8 - N° 10 - October 1971.

[31] N.D. HAM
Aerodynamic loading on a two-dimensional airfoil during dynamic stall
AIAA Journal Vol: 6 - N° 10 - October 1968

[32] J.J. PHILIPPE -M. SAGNER
Computations and Measurements of Aerodynamic Forces on an Oscillating Airfoil
AGARD CP n° 111 "Aerodynamics of Rotary wings" 1973.

[33] N. BAUDU - M. SAGNER - J. SOUQUET
Modelling Dynamic Stall of an Oscillating Airfoil
AAAF - 10th Applied Aerodynamics Colloquium, Lille, November 1973

[34] T. SARPKAYA
An analytical study of separated flow about circular cylinders
Trans. ASME, J. Basic Engineering 90-511 1968

[35] R.M. SCRUGGS - J.F. NASH - R.E. SINGLETON
Analysis of dynamic stall using unsteady boundary layer theory
NASA CR 2462 - October 1974

[36] IUTAM Symposium 1971 "Recent research on unsteady boundary layers"
Publ. : E.A. Eichelbrenner - Les Presses de l'Université de Laval - Québec - 1972

[37] R.B. KINNEY - W.R. SEARS
Unsteady Aerodynamics - Vol. 1 et 2
Editeur : Université d'Arizona - Tucson - 1975

[38] W.R. SEARS - D.P. TELIONIS
Boundary layer separation in unsteady flow
SIAM Journal on Applied Mathematics
Vol. 28 n° 1, January 1975

[39] V.C. PATEL - J.F. NASH
Unsteady turbulent boundary layers with flow reversal
Symposium on unsteady Aerodynamics - Tucson 1975 (réf.37) ; also NASA CR 2546, May 1975

[40] J. COUSTEIX - R. HOUDEVILLE - A. DESOPPER
Experimental results and calculating methods concerning transitional and turbulent boundary layers in unsteady flows
FDP AGARD meeting on Unsteady Aerodynamics - Ottawa - September 1977

[41] U.B. MEHTA - Z. LAVAN
Starting Vortex, Separation Bubbles and Stall : A Numerical Study of Laminar Unsteady Flow around an Airfoil -
Journal of Fluid Mechanics., Vol. 67, Part 2, January 1975

[42] U.B. MEHTA
Dynamic Stall of an Oscillating Airfoil
FDP AGARD meeting on Unsteady Aerodynamics
Ottawa - September 1977

[43] J.C. WU - N.L. SANKAR - S. SAMPATH
A Numerical Study of Unsteady Viscous Flows Around Airfoils
FDP AGARD meeting on Unsteady Aerodynamics
Ottawa - September 1977

[44] R.B. KINNEY
Two-Dimensional Viscous Flow Past on Airfoil in an Unsteady Airstream
FDP AGARD meeting on Unsteady Aerodynamics
Ottawa - September 1977

[45] J.S. SHAMROTH - J.P. KRESKOVSKY
A Weak Interaction Study of the Viscous Flow about Oscillating Airfoils
NASA CR 132 425, May 1974

[46] J.D. LANG
On predicting leading egde bubble bursting on an airfoil in unsteady incompressible flow
Cranfield Memo 109 - April 1976

[47] P. CRIMI
Dynamic Stall
AGARD - AG - 172 - November 1973

[48] P. CRIMI
Investigation of non linear inviscid and viscous flow effects in the analysis of dynamic stall
NASA CR - 2335 - February 1974

[49] P.V.K. PERUMAL - F. SISTO
Lift and Moment Prediction for an Oscillatory Airfoil with a Moving Separation Point.
Trans. ASME, Series A, Vol. 96, N° 4, October 1974 - on Journal of Engineering for Power - Paper n° 74-GT-28

[50] W.R. SEARS
Unsteady Motion of Airfoils with Boundary Layer Separation.
AIAA Journal - Vol. 14, N° 2 - February 76

[51] B. MASKEW, F.A. DVORAK
Investigation of Separation Models for the Prediction of Cl Max.
33rd Annual National Forum of the AHS - Washington - May 1977

[52] P.J. ARCIDIACONNO, F.D. CARTA, L.D. CASELLINI, H.L. ELMAN
Investigation of helicopter control loads induced by stall flutter.
USA AVLABLS TR 70-2 - March 1970

[53] F.O. CARTA, G.L. COMMERFORD, R.G. CARLSON, R.H. BLACKWELL
Investigation of airfoil dynamic stall and its influence a helicopter control loads.
USA AMRDL TR 72-51, September 1972

[54] F.O. CARTA
Unsteady normal force on an airfoil in a periodically stalled inlet flow
J. of Aircraft - Vol. 4 n° 5, 1967

[55] F.O. CARTA, L.B. CASELLINI, P.J. ARCIDIACONNO, H.L. ELMAN
Analytical study of helicopter rotor blade flutter
26th Annual National Forum AHS - June 1970

[56] F.O. CARTA, G.L. COMMERFORD, R.G. CARLSON
Determination of Airfoil and Rotor Blade Dynamic Stall Response
J. of the AHS - Vol 18 - N° 2 - April 73

[57] R.L. BIELAWA
Synthesized Unsteady Airfoil Data with Applications to Stall Flutter Calculations
31st Annual National Forum of the AHS, May 1975

[58] D. GROSS, F.D. HARRIS
Prediction of inflight stalled airloads from oscillating airfoil data
25th Annual National Forum - AHS - May 1969

[59] F.D. HARRIS - F.J. TARZANIN - R. FISHER
Rotor high speed performance - Theory versus Test.
J. of the AHS - Vol. 15 - N° 3 - July 1970

[60] F.D. TARZANIN
Prediction of control loads due to blade stall
J. of the AHS - Vol. 17 - N° 2 - April 1972

[61] R.E. GORMONT
A Mathematical Model of Unsteady Aerodynamics and Radial Flow for Application to Helicopter Rotors
USAAMRDL TR 72-67 - May 1973

[62] J.J. COSTES
Rotor Response Prediction with non linear Aerodynamics Loads on the Retreating Blade
Second European Rotorcraft and Powered Lift Aircraft Forum - Bückeburg - 20-22 September 1976, also : Recherche Aérospatiale N° 1975-3

[63] R.G. CARLSON - R.H. BLACKWELL - G.L. COMMERFORD - P.H. MIRICK
Dynamic stall modeling and correlation with experimental data on airfoils and rotors
AHS/NASA Ames - Spécialists' Meeting on Rotorcraft Dynamics - February 1974

[64] T.S. BEDDOES
A synthesis of unsteady aerodynamics effects including stall hysteresis
1st European Rotorcraft and Powered Lift Aircraft Forum - University of Southampton England, September 1975

[65] L.E. ERICSSON - J.P. REDING
Dynamic stall analysis in light of recent numerical and experimental results.
J. of Aircraft - Vol. 13 n° 4 - April 1976
(AIAA Paper 75-26 - January 1975).

[66] L.E. ERICSSON - J.P. REDING
Quasi-steady and transient dynamic stall characteristics
AGARD FDP Symposium on "Prediction of Aerodynamics Loading" - Ames - Sept. 1976

[67] L.E. ERICSSON - J.P. REDING
Unsteady airfoil stall, review and extension
J. of Aircraft - Vol. 8 N° 8 - August 1971

[68] L.E. ERICSSON - J.P. REDING
Dynamic stall of helicopter blades
J. of the AHS - Vol. 17 N° 1 - January 72

[69] L.E. ERICSSON - J.P. REDING
Stall flutter analysis
J. of Aircraft. vol. 10 N° 1 January 1973.

[70] L.E. ERICSSON
Dynamics effects of shock-induced flow separation
J. of Aircraft - February 1975

[71] L.E. ERICSSON - J.P. REDING
Scaling problems in dynamic tests of aircraft like configurations
AGARD FDP Symposium on "Unsteady Aerodynamics"
Ottawa - September 1977

[72] N.D. HAM
Aerodynamic loading on a two-dimensional airfoil during dynamic stall
AIAA Journal - Vol. 6 n° 10 - October 1968

[73] N.D. HAM - M.S. GARELICK
Dynamic stall considerations in helicopter rotors
J. of the AHS - Vol. 13 N° 2 - April 1968

[74] W.JOHNSON
The effect of dynamic stall on the response and airloading of helicopter rotor blades
J. of AHS - Vol. 14 n° 2, april 1969

[75] W. JOHNSON
Comparison of three methods for calculating of helicopter rotor blade loading and stresses due to stall
NASA TN D-7833 - November 1974

[76] W. JOHNSON - N.D. HAM
On the mechanism of dynamic stall
J. of AHS, Vol. 17 - n° 4 - October 1974

[77] A.J. LANDGREBE, R.C. MOFFIT, D.R. CLARK
Aerodynamic Technology for Advanced Rotorcraft
Journal of the American Helicopter Society
Part 1 - Vol. 22 n° 2 - April 1977
Part 2 - Vol. 22 n° 3 - July 1977